OPEN ACCESS
CellPress

Cell Reports
Article

5-Hydroxymethylcytosine Plays a Critical Role in Glioblastomagenesis by Recruiting the CHTOP-Methylosome Complex

Hiroki Takai,[1] Koji Masuda,[2] Tomohiro Sato,[1] Yuriko Sakaguchi,[3] Takeo Suzuki,[3] Tsutomu Suzuki,[3] Ryo Koyama-Nasu,[1] Yukiko Nasu-Nishimura,[1] Yuki Katou,[2] Haruo Ogawa,[4] Yasuyuki Morishita,[5] Hiroko Kozuka-Hata,[6] Masaaki Oyama,[6] Tomoki Todo,[7] Yasushi Ino,[7] Akitake Mukasa,[7] Nobuhito Saito,[7] Chikashi Toyoshima,[4] Katsuhiko Shirahige,[2] and Tetsu Akiyama[1,*]

[1]Laboratory of Molecular and Genetic Information, Institute of Molecular and Cellular Biosciences, The University of Tokyo, 1-1-1, Yayoi, Bunkyo-ku, Tokyo 113-0032, Japan

[2]Laboratory of Genome Structure and Function, Research Center for Epigenetic Disease, Institute of Molecular and Cellular Biosciences, The University of Tokyo, 1-1-1, Yayoi, Bunkyo-ku, Tokyo 113-0032, Japan

[3]Department of Chemistry and Biotechnology, Graduate School of Engineering, The University of Tokyo, 7-3-1, Hongo, Bunkyo-ku, Tokyo 113-8656, Japan

[4]Laboratory of Membrane Proteins, Center for Structural Biology of Challenging Proteins, Institute of Molecular and Cellular Biosciences, The University of Tokyo, 1-1-1, Yayoi, Bunkyo-ku, Tokyo 113-0032, Japan

[5]Department of Molecular Pathology, Graduate School of Medicine, The University of Tokyo, 7-3-1, Hongo, Bunkyo-ku, Tokyo 113-0033, Japan

[6]Medical Proteomics Laboratory, Institute of Medical Science, The University of Tokyo, 4-6-1, Shirokanedai, Minato-ku, Tokyo 108-8639, Japan

[7]Department of Neurosurgery, The University of Tokyo Hospital, 7-3-1, Hongo, Bunkyo-ku, Tokyo 113-8655, Japan

*Correspondence: akiyama@iam.u-tokyo.ac.jp

http://dx.doi.org/10.1016/j.celrep.2014.08.071

This is an open access article under the CC BY-NC-ND license (http://creativecommons.org/licenses/by-nc-nd/3.0/).

SUMMARY

The development of cancer is driven not only by genetic mutations but also by epigenetic alterations. Here, we show that TET1-mediated production of 5-hydroxymethylcytosine (5hmC) is required for the tumorigenicity of glioblastoma cells. Furthermore, we demonstrate that chromatin target of PRMT1 (CHTOP) binds to 5hmC. We found that CHTOP is associated with an arginine methyltransferase complex, termed the methylosome, and that this promotes the PRMT1-mediated methylation of arginine 3 of histone H4 (H4R3) in genes involved in glioblastomagenesis, including *EGFR*, *AKT3*, *CDK6*, *CCND2*, and *BRAF*. Moreover, we found that CHTOP and PRMT1 are essential for the expression of these genes and that CHTOP is required for the tumorigenicity of glioblastoma cells. These results suggest that 5hmC plays a critical role in glioblastomagenesis by recruiting the CHTOP-methylosome complex to selective sites on the chromosome, where it methylates H4R3 and activates the transcription of cancer-related genes.

INTRODUCTION

Covalent modifications of DNA and histones influence transcriptional activity and the timing of DNA replication, thereby regulating cell proliferation, survival, self-renewal, and tumorigenesis (Goldberg et al., 2007; Sasaki and Matsui, 2008). Methylation at the five position of cytosine is one of the most abundant modifications of DNA and is required for the regulation of gene expression, genome stability, and genomic imprinting (Baylin and Jones, 2011). This modification is mediated by the DNA methyltransferase family of proteins and occurs predominantly in CpG dinucleotides (Bird, 2001; Jones, 2012). It has recently been shown that 5mC is oxidized to 5-hydroxymethylcytosine (5hmC) by the ten-eleven translocation (TET) family of Fe(II) and 2-oxoglutarate-dependent DNA dioxygenases, TET1∼TET3 (He et al., 2011; Ito et al., 2011; Tahiliani et al., 2009). 5hmC is found in diverse cell types and developmental stages, including embryonic stem cells and Purkinje cells (Cimmino et al., 2011; Dawlaty et al., 2013; Guo et al., 2011; Hahn et al., 2013; Koh et al., 2011; Wu and Zhang, 2014). More recently, 5hmC has been shown to be successively oxidized to 5-formylcytosine (5fC) and 5-carboxylcytosine (5caC) by the TET family of enzymes (He et al., 2011; Ito et al., 2011; Shen et al., 2014; Wu and Zhang, 2014). 5hmC, 5fC, and 5caC are assumed to be intermediates in DNA demethylation, and 5fC and 5caC can be converted to unmodified cytosine by thymine-DNA glycosylase (TDG) and by the base excision repair pathway (Guo et al., 2011; He et al., 2011).

It has recently been shown that 5hmC acts not only as an intermediate of DNA demethylation but also as an epigenetic mark that recruits DNA-binding proteins. For example, it has been shown that the Mbd3/NURD complex regulates expression of 5hmC-marked genes in embryonic stem cells (ESCs) (Yildirim et al., 2011). It has also been reported that MeCP2 binds to 5hmC

CrossMark

that is enriched within active genes as well as accessible chromatin in the nervous system (Mellén et al., 2012). More recently, it has been shown that 5mC, 5hmC, 5fC, and 5caC recruit distinct sets of proteins in a dynamic and cell-type-dependent manner (Spruijt et al., 2013). This result suggests that 5hmC, 5fC, and 5caC may recruit transcription regulators in certain cell types, as well as DNA repair proteins that may also be involved in DNA demethylation.

5hmC and the TET family of enzymes function in a diverse set of biological processes, including embryogenesis and differentiation (Cimmino et al., 2011; Dawlaty et al., 2013; Guo et al., 2011; Hahn et al., 2013; Koh et al., 2011; Wu and Zhang, 2014). 5hmC and TET family enzymes also play critical roles in the development of cancer (Cimmino et al., 2011). TET1 was first identified as part of a fusion gene with mixed lineage leukemia in patients with acute myeloid leukemia (AML) (Ono et al., 2002). Furthermore, it has been reported that TET2 is frequently inactivated by mutations or deletions in various myeloid leukemias, resulting in the downregulation of 5hmC levels (Delhommeau et al., 2009). It is also known that isocitrate dehydrogenase 1 and 2 (IDH1 and IDH2) are mutated in AML, glioma, sarcoma, and melanoma (Dang et al., 2009; Parsons et al., 2008; Ward et al., 2010). Whereas wild-type IDHs generate α-ketoglutarate, mutated IDHs produce an oncometabolite, 2-hydroxyglutarate, which inhibits the TET family of enzymes and thereby interferes with the conversion of 5mC to 5hmC (Figueroa et al., 2010; Xu et al., 2011). More recently, it has been reported that transcriptional downregulation rather than mutation of TET family enzymes or IDH can result in the depletion of 5hmC in many cancers, including melanoma, breast, lung, and prostate cancers (Hsu et al., 2012; Lian et al., 2012).

In the present study, we examined the levels of 5hmC and TET1 in glioblastoma, the most malignant type of brain tumor, which has a median survival of approximately 1 year (Furnari et al., 2007; Stupp et al., 2005). We found that, in contrast to previous studies of other tumor types (Cimmino et al., 2011), proneural glioblastoma contain high levels of 5hmC and TET1 and that TET1-mediated production of 5hmC is required for glioblastomagenesis. Furthermore, we found that 5hmC recruits chromatin target of PRMT1 (CHTOP) associated with the methylosome (Friesen et al., 2001), which methylates arginine 3 on histone H4 (H4R3) and activates the transcription of cancer-related genes.

RESULTS

Glioblastoma Cells Contain Elevated Levels of 5hmC and TET1

Glioblastoma cells cultured in serum-free conditions form spheres and retain stem-cell-like properties and tumorigenicity (Lee et al., 2006). We have previously described the isolation and culture of glioblastoma cells from seven patients, designated GB1∼GB5, GB11, and GB13 (Koyama-Nasu et al., 2013). DNA array analysis revealed that GB2∼GB5, GB11, and GB13 resembled proneural glioblastoma cells, whereas GB1 resembled the mesenchymal type (Lottaz et al., 2010; Figure S1A). Furthermore, we performed quantitative RT-PCR (qRT-PCR) analyses to examine the expression levels of marker genes indicating subtypes of glioblastoma in patient samples (GBM3–GBM7) as well as in glioblastoma cell lines (GB1–GB5, GB8, and GB21). We found that glioblastoma patient samples and cell lines were classified into four subtypes: proneural, neural, classical, and mesenchymal (Figure S1B). In addition, we found that the glioblastoma cell lines and patient samples used in this study do not have mutations in either IDH1 (R132) or IDH2 (R172; Figure S1C).

Previous studies have reported that 5hmC was strongly depleted in tissue stem cell compartments and human cancers (Haffner et al., 2011; Hsu et al., 2012; Kraus et al., 2012; Lian et al., 2012; Müller et al., 2012; Orr et al., 2012). However, our dot blot analysis showed that GB2∼GB5, GB11, and GB13 cells, but not GB1 cells, contained elevated levels of 5hmC compared to HeLa, U87MG, and human neural progenitor cell lines (hNPCs) (Figure 1A). Furthermore, absolute mRNA quantification using qRT-PCR analyses revealed that TET1 expression levels were significantly higher than those of the other TET family members (TET2 and TET3) in GB2∼GB5, GB11, and GB13 cells and in hNPCs, but not in GB1 cells (Figure 1B). Moreover, using a stable isotope-labeled 5hmC as an internal standard, we quantified the genomic content of 5hmC in glioblastoma cells by liquid chromatography-mass spectrometry (LC-MS). We found that 5hmC accounts for about one percent of all genomic cytosines in glioblastoma cells (Figure 1C). We also performed dot blot analysis of glioblastoma patient samples and found that the levels of 5hmC and TET1 expression were upregulated in proneural glioblastoma, but not in other subtypes (Figures 1D, 1E, and S1D–S1F). Thus, upregulation of TET1 may be responsible for the elevated levels of 5hmC in the proneural subtypes.

TET1-Mediated Production of 5hmC Is Required for Glioblastomagenesis

We next examined whether the TET family of genes is involved in the proliferation and tumorigenicity of glioblastoma cells. Infection of GB2 cells with a lentivirus expressing a small hairpin RNA (shRNA) or small interfering RNA (siRNA) targeting TET1 resulted in a significant decrease in their growth (Figures 2A and S2A). Knockdown of TET1 also suppressed sphere formation of GB3∼GB5 cells (Figure 2B). Furthermore, we found that overexpression of wild-type, but not of catalytic mutant TET1, restored the growth and sphere formation of GB2 cells in which TET1 had been knocked down (Figures 2A, 2C, and S2B). Consistent with these results, overexpression of wild-type TET1, but not of mutant TET1, restored the decreased levels of 5hmC caused by knockdown of TET1 (Figure S2C). These results suggest that TET1 is important for the proliferation of glioblastoma cells. We next infected GB2 cells with lentivirus-expressing shRNAs directed against TET1 and intracranially transplanted these into immunodeficient mice. Mice receiving the shRNA-expressing GB2 cells survived significantly longer than those receiving GB2 cells infected with a control lentivirus (Figure 2D). Histopathological analysis of tumor xenografts demonstrated that knockdown of TET1 inhibited glioblastoma progression, whereas control GB2 cells formed invasive glioblastoma (Figure 2E). Moreover, we found that overexpression of TET1 restored the tumorigenicity of GB2 cells in which TET1 had been knocked down (Figure 2D). These results suggest that

OPEN ACCESS
CellPress

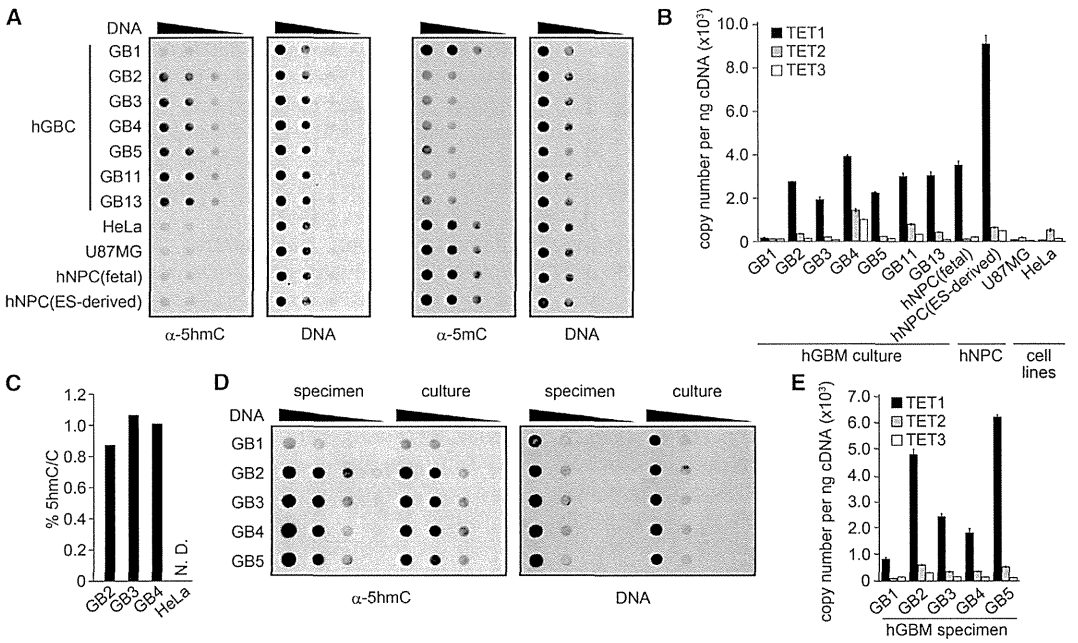

Figure 1. 5hmC and TET1 Levels in Human Glioblastoma Cells

(A) Dot blot analysis of genomic 5hmC and 5mC in human glioblastoma cells and NPCs.

(B) Absolute expression levels of the TET family of genes were determined by qRT-PCR. Copy numbers were calculated according to the standard curves generated by known quantities of plasmids containing the TET family of genes. Data show the means ± SD of three independent experiments.

(C) LC-MS quantification of 5hmC in genomic DNA isolated from glioblastoma cells and HeLa cells. N.D., not detected.

(D) Dot blot analysis of genomic 5hmC in primary glioblastoma samples and cultured cells.

(E) Absolute expression levels of the TET family of genes in primary glioblastoma samples as determined by qRT-PCR. Data show the means ± SD of three independent experiments.

See also Figure S1.

TET1 plays a critical role in the tumorigenicity of glioblastoma cells.

TET1-Catalyzed Enrichment of 5hmC Is Critical for the Expression of Cancer-Related Genes

To identify hydroxymethylated loci on a genomic scale, we immunoprecipitated 5-hydroxymethylated DNA using a 5hmC-specific antibody and analyzed the DNA by high-throughput sequencing (hMeDIP-seq). We found that the number of 5hmC peaks was greater in the genome of GB2 cells compared to the hNPC genome (Figure 3A). 5hmC was relatively enriched within the intragenic regions and promoters, as previously observed in mouse embryonic stem cells (Figures 3B and 3C). Gene ontology analysis revealed that genes encoding components of cancer-related signaling pathways and neuronal functions are overrepresented among the hydroxymethylated genes (Table S1). Furthermore, we identified intragenic 5hmC peaks in the *EGFR*, *AKT3*, *CDK6*, *CCND2*, and *BRAF* genes (Figure 3D). hMeDIP-qPCR assays to detect 5hmC in these five genes confirmed the results of hMeDIP-seq analyses (Figure 3E). By contrast, we could not detect 5hmC enrichment in these genes in hNPCs. To elucidate the significance of elevated 5hmC content in these genes in glioblastoma cells, we examined the effect of TET1 knockdown on their expression. We found that knockdown of TET1 resulted in decreased expression of these five genes (Figure 3F). Furthermore, we found that overexpression of wild-type, but not of mutated, TET1 restored the expression of these genes in GB2 cells in which TET1 had been knocked down. Thus, TET1-mediated enrichment of 5hmC may be critical for their expression. EGFR and AKT3 are core components of the RTK/RAS/PI(3)K-signaling pathway, whereas CDK6 and CCND2 are key regulators of the RB-signaling pathway. These two signaling pathways, together with the p53-signaling pathway, are known to be frequently altered in glioblastoma. Our results therefore suggest that the TET1-catalyzed enrichment of 5hmC in these genes may drive the tumorigenicity of glioblastomas.

5hmC Interacts with CHTOP in Glioblastoma Cells

Based on the above findings, we hypothesize that 5hmC is not just an intermediate in DNA demethylation but functions as a *cis*-acting modulator of gene activity. Consistent with this notion, it has recently been reported that enrichment of 5hmC is not associated with DNA demethylation during neurogenesis (Hahn et al., 2013). To test our hypothesis, we attempted to identify proteins that interact with 5hmC. We prepared synthetic double-stranded DNA oligonucleotides that contain three modified CpG residues (Figure S3A). We incubated

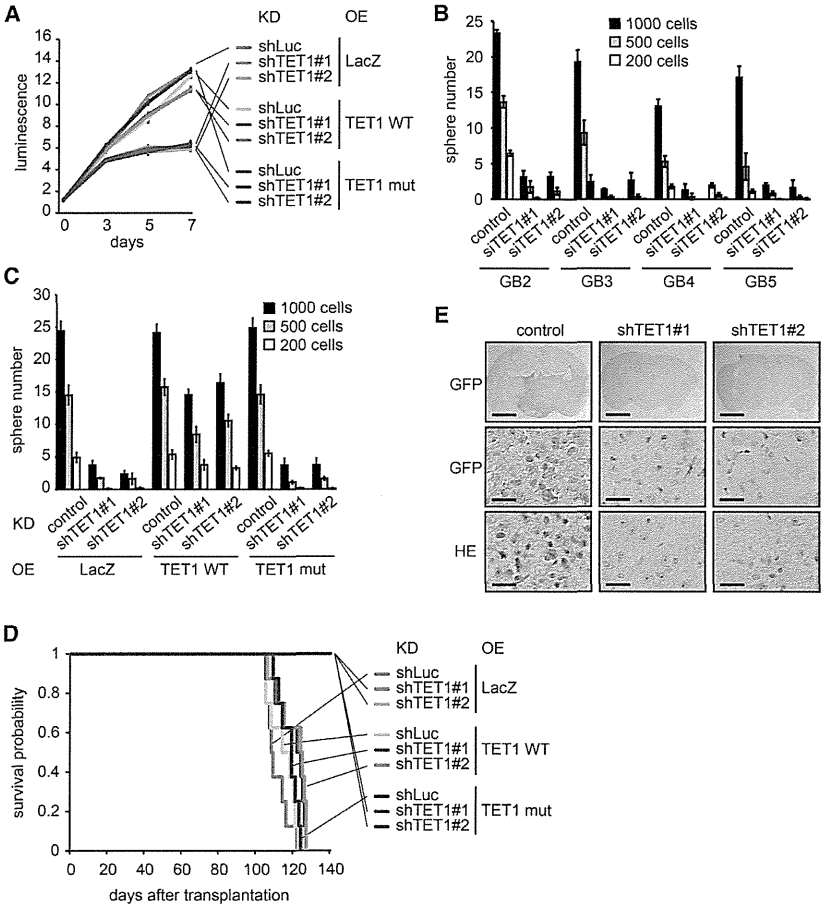

Figure 2. TET1 Is Required for the Tumorigenicity of Glioblastoma Cells

(A) Growth curves of GB2 cells infected with a lentivirus expressing shRNA targeting TET1 and/or a lentivirus expressing wild-type or mutant TET1. Data show the means ± SD of three independent experiments. KD, knockdown. OE, overexpression.

(B) The numbers of spheres of glioblastoma cells transfected with siRNA targeting TET1. Data show the means ± SD of three independent experiments.

(C) The number of spheres of GB2 cells infected with a lentivirus expressing shRNA targeting TET1 and/or a lentivirus expressing wild-type or mutant TET1. Data show the means ± SD of three independent experiments.

(D) Kaplan-Meier survival curves of mice transplanted with 1.0×10^4 GB2 cells infected with a lentivirus expressing shRNA targeting TET1 or a lentivirus expressing wild-type or mutant TET1.

(E) Histological examination of tumors developed in the mice in (D). At day 100, tissue sections were stained with hematoxylin and eosin (HE) or anti-GFP antibody. The scale bars represent 2 mm (upper panels) and 50 μm (lower panels).

See also Figure S2.

3′-biotin-tagged oligonucleotides with nuclear extracts from GB2 cells. The bound proteins were precipitated with streptavidin-Dynabeads and subjected to LC-MS (Figure S3B). Among the coprecipitated proteins identified (Table S2), we focused our attention on CHTOP, because it preferentially bound to the 5hmC-containing oligonucleotide versus the unmodified or 5mC-containing oligonucleotide (Figure 4A, upper panel). CHTOP is a chromatin-associated protein that is involved in transcriptional regulation. It contains a glycine- and arginine-rich (GAR) region, which interacts with RNA or DNA directly or in combination with other nucleotide-binding proteins (Rajyaguru and Parker, 2012). We generated recombinant CHTOP using a baculovirus system (Figure S3C) and confirmed that CHTOP preferentially bound to 5hmC in vitro (Figure 4A, lower panel). Moreover, we performed electrophoretic mobility shift assays and found that CHTOP preferentially binds to the 5hmC-containing oligonucleotide (Figure S3D, left panel). Addition of an anti-CHTOP antibody induced a supershift of the band (Figure S3D, middle panel), suggesting that the band detected may indeed represent a complex consisting of CHTOP and the 5hmC-containing oligonucleotide. By contrast, MBD1 specifically interacted with the 5mC-containing oligonucleotide (Figure S3D, right panel).

CHTOP was first identified as a target of protein arginine methyltransferases, especially PRMT1 and PRMT5 (van Dijk et al., 2010; Zullo et al., 2009). PRMT1 catalyzes the generation of both monomethylarginine and asymmetrical dimethylarginine residues, whereas PRMT5 generates monomethylarginine and symmetrical dimethylarginine residues (Bedford and Clarke, 2009; Martin and Zhang, 2005). Immunoblotting analysis of CHTOP with antibody against asymmetrical or symmetrical dimethylarginine revealed that CHTOP is asymmetrically, but not symmetrically, dimethylated at arginine residues in human embryonic kidney 293FT (HEK293FT) cells (Figure 4B). Knockdown of PRMT1 using siRNA resulted in a reduction in the asymmetrical methylation of arginine residues in CHTOP. PRMT1 knockdown also led to a reduction in CHTOP, especially the upper band of the doublet. In addition, as reported previously (van Dijk et al., 2010), incubation of purified glutathione S-transferase (GST)-PRMT1 and GST-CHTOP in vitro resulted in the asymmetrical methylation of CHTOP (Figure 4C). The asymmetrical methylation of CHTOP retarded its migration, suggesting that the upper band of CHTOP detected in vivo may represent the asymmetrically dimethylated form. We speculate that arginine methylation of CHTOP may increase its molecular weight and reduce its positive charge, causing its retarded migration in SDS-PAGE.

We next examined the effect of arginine methylation on the 5hmC-binding activity of CHTOP. We found that knockdown of PRMT1 suppressed the 5hmC-binding activity of CHTOP (Figure 4D). By contrast, knockdown of PRMT5 barely affected the arginine methylation or 5hmC-binding ability of

OPEN ACCESS
CellPress

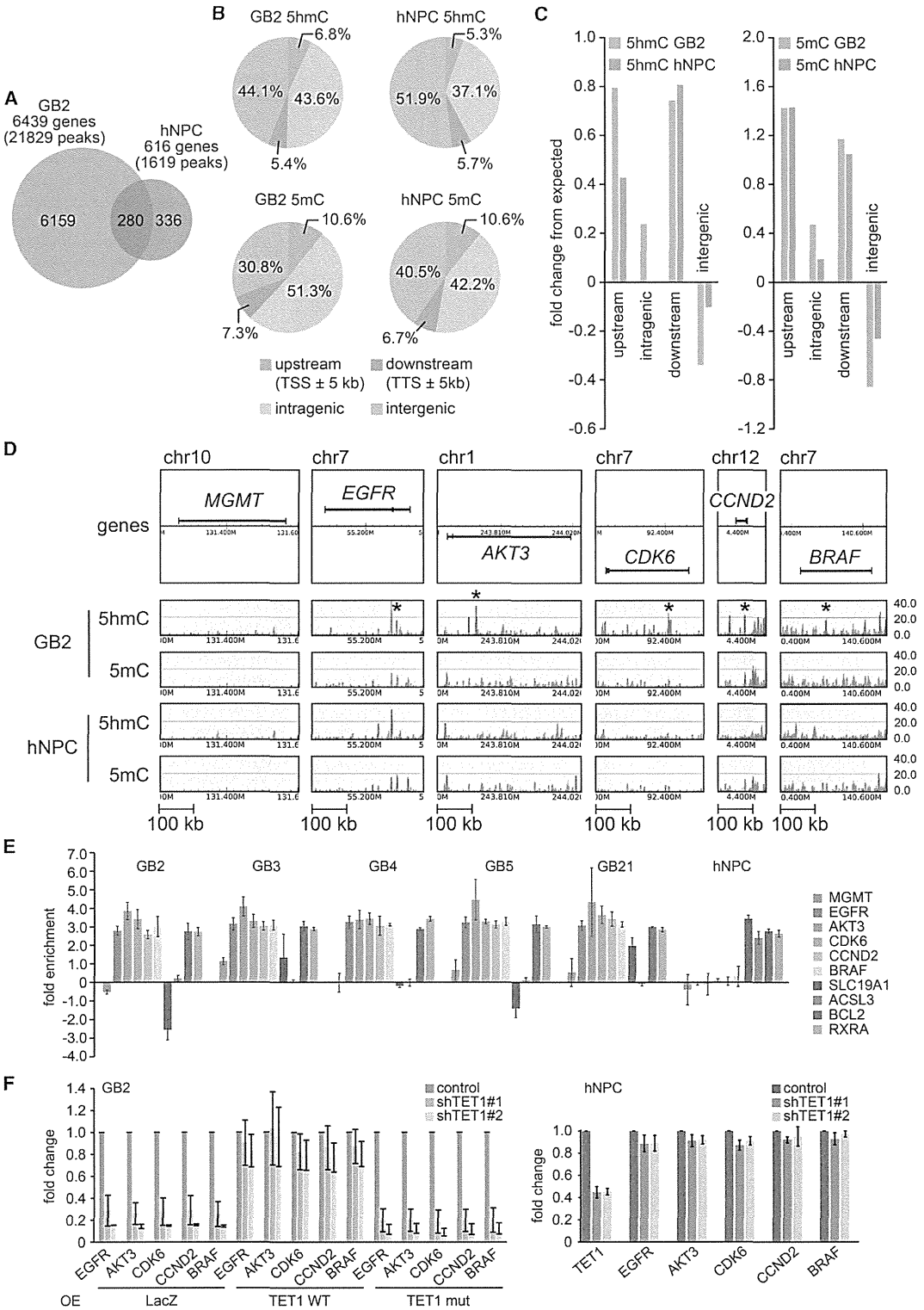

(legend on next page)

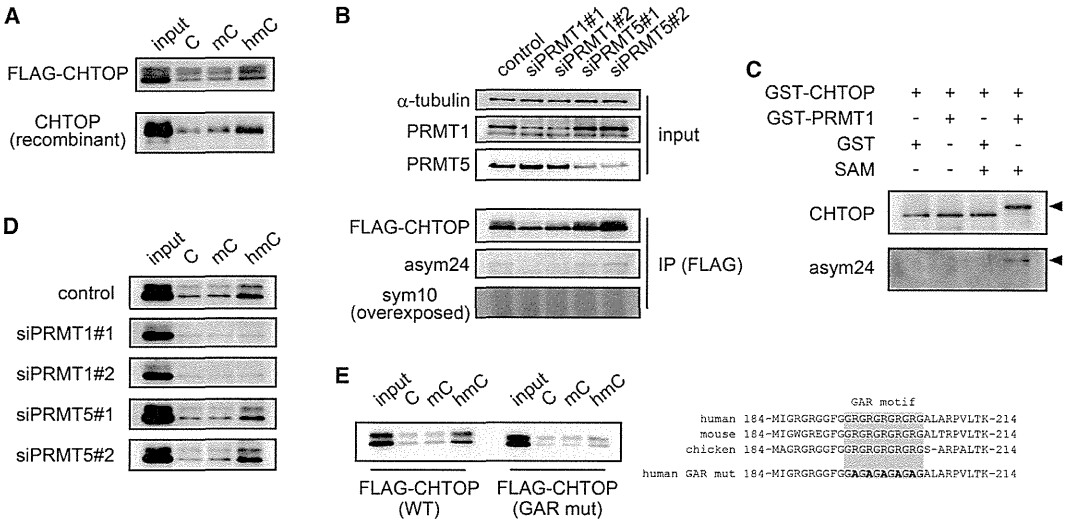

Figure 4. 5hmC Is Associated with CHTOP in Glioblastoma Cells

(A) CHTOP preferentially binds to 5hmC. Biotin-tagged oligonucleotides containing the indicated nucleotide modifications were incubated with lysates from HEK293FT cells transfected with FLAG-CHTOP (upper panel) or recombinant CHTOP generated using the baculovirus system (lower panel). C, unmodified cytosine; mC, 5-methylcytosine; hmC, 5-hydroxymethylcytosine.

(B) CHTOP is asymmetrically dimethylated by PRMT1, but not symmetrically by PRMT5. Lysates from HEK293FT cells transfected with FLAG-CHTOP and siRNA targeting PRMT1 or PRMT5 were subjected to immunoprecipitation with anti-FLAG antibody followed by immunoblotting with the indicated antibodies: asym24, antibody against asymmetrically dimethylated arginine; sym10, antibody against symmetrically dimethylated arginine.

(C) PRMT1 asymmetrically dimethylates CHTOP in vitro. GST-CHTOP was incubated with GST-PRMT1 in vitro and subjected to immunoblotting analysis with the indicated antibodies. The upper band indicated by the arrowhead represents asymmetrically dimethylated CHTOP.

(D) PRMT1-mediated methylation of CHTOP is required for its binding to 5hmC. Lysates from HEK293FT cells transfected with FLAG-CHTOP and siRNA against PRMT1 or PRMT5 were subjected to pull-down assays as in (A).

(E) CHTOP binds to 5hmC via its GAR motif. Lysates from HEK293FT cells transfected with FLAG-tagged wild-type or GAR mutant CHTOP were subjected to pull-down assays as in (A). Sequences of the GAR motif of CHTOP are shown in the right panel. WT, wild-type.

See also Figure S3 and Table S2.

CHTOP. Consistent with these results, a mutant CHTOP, in which five arginine residues in the GAR region were replaced with alanine, did not interact with 5hmC (Figure 4E). These results suggest that PRMT1-mediated arginine methylation is critical for the 5hmC-binding activity of CHTOP.

CHTOP Associated with 5hmC Recruits the Methylosome

To further elucidate the function of CHTOP, we analyzed its associated proteins in cell extracts. FLAG-CHTOP was overexpressed in HEK293FT cells and immunoprecipitated with anti-FLAG antibody followed by SDS-PAGE and silver staining. When coimmunoprecipitated proteins were analyzed by LC-MS, we found that PRMT1, PRMT5, methylosome protein 50 (MEP50), and enhancer of rudimentary homolog (ERH) were associated with CHTOP (Figure 5A; Table S3). Pull-down assays using lysates from GB2 cells infected with a lentivirus expressing wild-type or GAR mutant CHTOP confirmed that CHTOP was associated with these proteins (Figure 5B). Furthermore, we found that these proteins preferentially bind to 5hmC-containing oligonucleotides (Figure 5C). These proteins are components of an arginine methyltransferase complex, termed the methylosome (Friesen et al., 2001), which is involved in several cellular processes, including the

Figure 3. 5hmC Is Enriched in Genes Involved in Glioblastomagenesis

(A) Venn diagram showing the number of 5-hydroxymethylated genes in GB2 cells and NPCs. (h)MeDIP-seq was performed with cell extracts using antibodies specific for 5mC or 5hmC.

(B) Association of all peaks identified with various genomic features.

(C) 5hmC and 5mC are enriched in intragenic and upstream regions in GB2 cells.

(D) 5mC and 5hmC profiles of the genes involved in glioblastomagenesis. Regions in which signals were significantly enriched are marked in red. Asterisks indicate the peaks confirmed by hMeDIP-qPCR in (E).

(E) hMeDIP-qPCR assays were performed with glioblastoma cells and NPCs using anti-5hmC antibody. SLC19A1 and ACSL3 are positive controls for NPCs. BCL2 and RXRA are positive controls for both glioblastoma cells and NPCs. Data show the means ± SD of three independent experiments.

(F) qRT-PCR analysis of the indicated genes in GB2 cells and NPCs infected with a lentivirus expressing shRNA targeting TET1 and/or a lentivirus expressing wild-type or mutant TET1. Data are the mean ± SD of three independent experiments. OE, overexpression.

See also Table S1.

OPEN ACCESS
CellPress

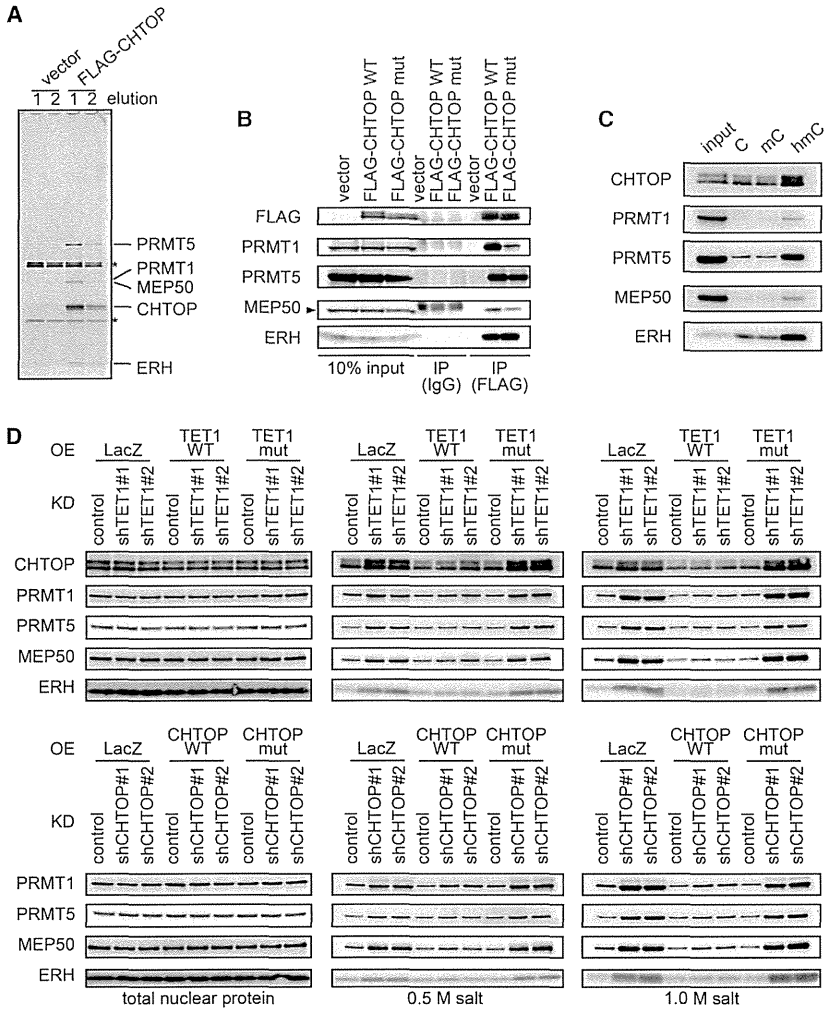

Figure 5. CHTOP Associated with the Methylosome Binds to 5hmC

(A) CHTOP is associated with the methylosome. Lysates from HEK293FT cells transfected with FLAG-CHTOP were subjected to immunoprecipitation with anti-FLAG antibody followed by SDS-PAGE and silver staining, and coprecipitated proteins were identified by mass spectrometry. Asterisks indicate immunoglobulin chains.

(B) CHTOP is associated with the methylosome in GB2 cells. The immunoprecipitates prepared as in (A) were subjected to immunoblotting analysis with the indicated antibodies.

(C) CHTOP and the methylosome preferentially bind to 5hmC in GB2 cells.

(D) Immunoblotting analysis of methylosome components extracted with salt buffer from the chromatin fractions prepared from GB2 cells infected with a lentivirus expressing the indicated shRNAs and/or a lentivirus expressing wild-type or mutant TET1 (upper panels) or CHTOP (lower panels). KD, knockdown.

See also Figure S4 and Table S3.

regulation of gene expression and RNA processing. Of particular note, it has been reported that PRMT1-mediated dimethylation of H4R3 is important for subsequent histone modifications such as acetylation and thereby is involved in modulating transcriptional activation (Huang et al., 2005; Wang et al., 2001).

To examine whether CHTOP is required for the association of the methylosome with chromatin, chromatin samples prepared from GB2 cells were incubated with NaCl and extracted proteins were analyzed by immunoblotting analysis (Meshorer et al., 2006). We found that knockdown of CHTOP resulted in increased amounts of PRMT1, PRMT5, MEP50, and ERH extracted from the chromatin fraction (Figures 5D, S4A, and S4B). We also found that knockdown of TET1 led to the increased extraction of these proteins, as well as increased extraction of CHTOP. In addition, the increased extraction of these proteins caused by knockdown of TET1 or CHTOP could be suppressed by overexpression of wild-type TET1 or CHTOP, but not of mutant TET1 or CHTOP. These results suggest that CHTOP associated with 5hmC functions as a recruiter of the methylosome.

H4R3 Is Methylated by PRMTs in a CHTOP- and/or TET1-Dependent Manner

We next investigated whether H4R3 is methylated by PRMTs in a CHTOP- and/or TET1-dependent manner. Immunoblotting analysis revealed that knockdown of either TET1 or CHTOP resulted in a reduction in the amounts of both H4R3me2a and H4R3me2s (Figure 6A). We also performed chromatin immunoprecipitation (ChIP) assays with antibodies against PRMT1, PRMT5, H4R3me2a, and H4R3me2s. We found that these are associated with the *EGFR*, *AKT3*, *CDK6*, *CCND2*, and *BRAF* genes, but not the *HPRT1* gene (Figure 6B). Knockdown of either CHTOP or TET1 reduced the association of PRMT1 and PRMT5 with these genes (Figure 6B). Furthermore, we found that knockdown of either CHTOP or TET1 resulted in decreases in both the asymmetrical and symmetrical dimethylation of H4R3 (Figure 6B), whereas knockdown of PRMT1 or PRMT5 led to a decrease in the asymmetrical or symmetrical dimethylation of H4R3, respectively (Figure S5A). We also found that knockdown of either TET1 or CHTOP led to an increase in the trimethylation of H3K27, whereas the trimethylation of H3K36 and the acetylation of H4 were not affected (Figure S5B). Consistent with these results, knockdown of either CHTOP or PRMT1 suppressed the expression of these genes (Figures 6C and 6D), whereas knockdown of PRMT5 barely changed their expression, except for *CCND2*.

Consistent with the above findings, RNA sequencing (RNA-seq) analyses revealed that knockdown of TET1,

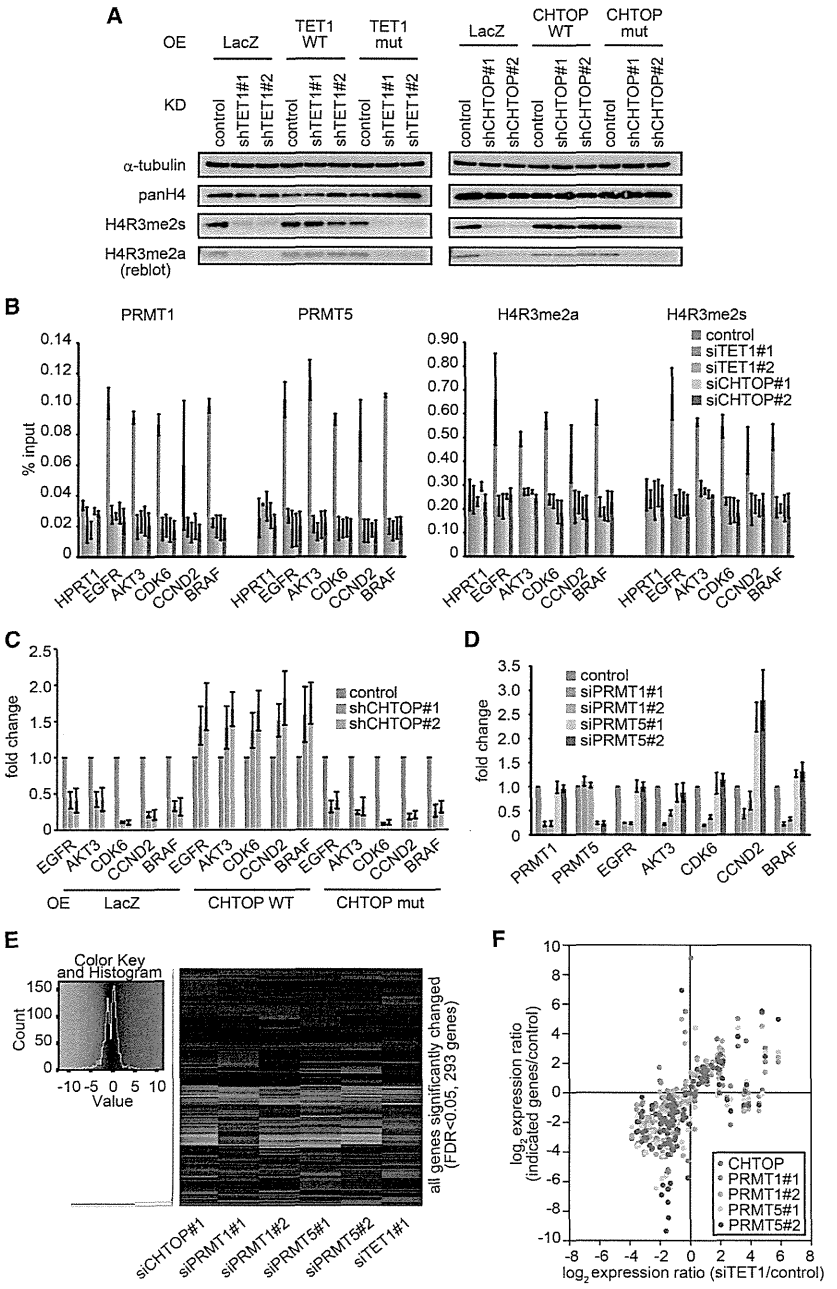

Figure 6. The CHTOP-Methylosome Complex Associated with 5hmC Methylates H4R3 and Transactivates Cancer-Related Genes

(A) Immunoblotting analysis of H4R3me2a and H4R3me2s in GB2 cells infected with a lentivirus expressing the indicated shRNAs and/or a lentivirus expressing wild-type or mutant TET1 (left panels) or CHTOP (right panels).

(B) PRMTs and H4R3me2 are associated with 5hmC-enriched loci in a TET1- and CHTOP-dependent manner. ChIP assays were performed with GB2 cells transfected with the indicated siRNAs. Data show the means ± SD of three independent experiments.

(C) qRT-PCR analyses of the indicated genes were performed using GB2 cells infected with a lentivirus expressing shRNA targeting CHTOP and/or a lentivirus expressing wild-type or mutant CHTOP. Data show the means ± SD of three independent experiments.

(D) qRT-PCR analyses of the indicated genes were performed using GB2 cells transfected with siRNA targeting PRMT1 or PRMT5. Data show the means ± SD of three independent experiments.

(E) RNA-seq analysis of GB2 cells transfected with the indicated siRNAs.

(F) Scatterplot comparing transcriptome between TET1 knockdown cells and CHTOP, PRMT1, or PRMT5 knockdown cells. Genes whose expression was significantly changed are shown.

See also Figure S5.

CHTOP Is Required for Maintaining 5hmC Levels

We next examined the expression levels of CHTOP in glioblastoma cells and hNPCs. We found that GB2~GB5, GB11, and GB13 cells, but not GB1 cells, express somewhat higher levels of CHTOP than hNPCs (Figure S6A). Furthermore, we found that knockdown of CHTOP results in a reduction in global 5hmC levels in GB2 cells (Figure S6B). We have also found that overexpression of wild-type, but not of GAR mutant, CHTOP restores 5hmC levels. These results suggest that CHTOP is required for maintaining 5hmC levels and that upregulation of CHTOP as well as TET1 is responsible for the elevated levels of 5hmC in glioblastoma cells. This may be one of the reasons why 5hmC levels are not elevated in hNPCs, in which only TET1, but not CHTOP, are upregulated.

CHTOP, PRMT1, or PRMT5 resulted in similar changes in gene-expression patterns in GB2 cells (Figures 6E and S5C) and that the gene-expression profile of TET1 knockdown cells strongly correlated with the profiles of cells in which the other genes were knocked down (Figure 6F). In addition, we found that 5hmC was overrepresented in the promoters and intragenic regions of approximately 30% of genes whose expression was significantly changed (false discovery rate < 0.05).

CHTOP Is Required for the Tumorigenicity of Glioblastoma Cells

Finally, we investigated the importance of CHTOP in the proliferation and tumorigenicity of glioblastoma cells. We found that knockdown of CHTOP led to decreases in sphere formation of

OPEN ACCESS
CellPress

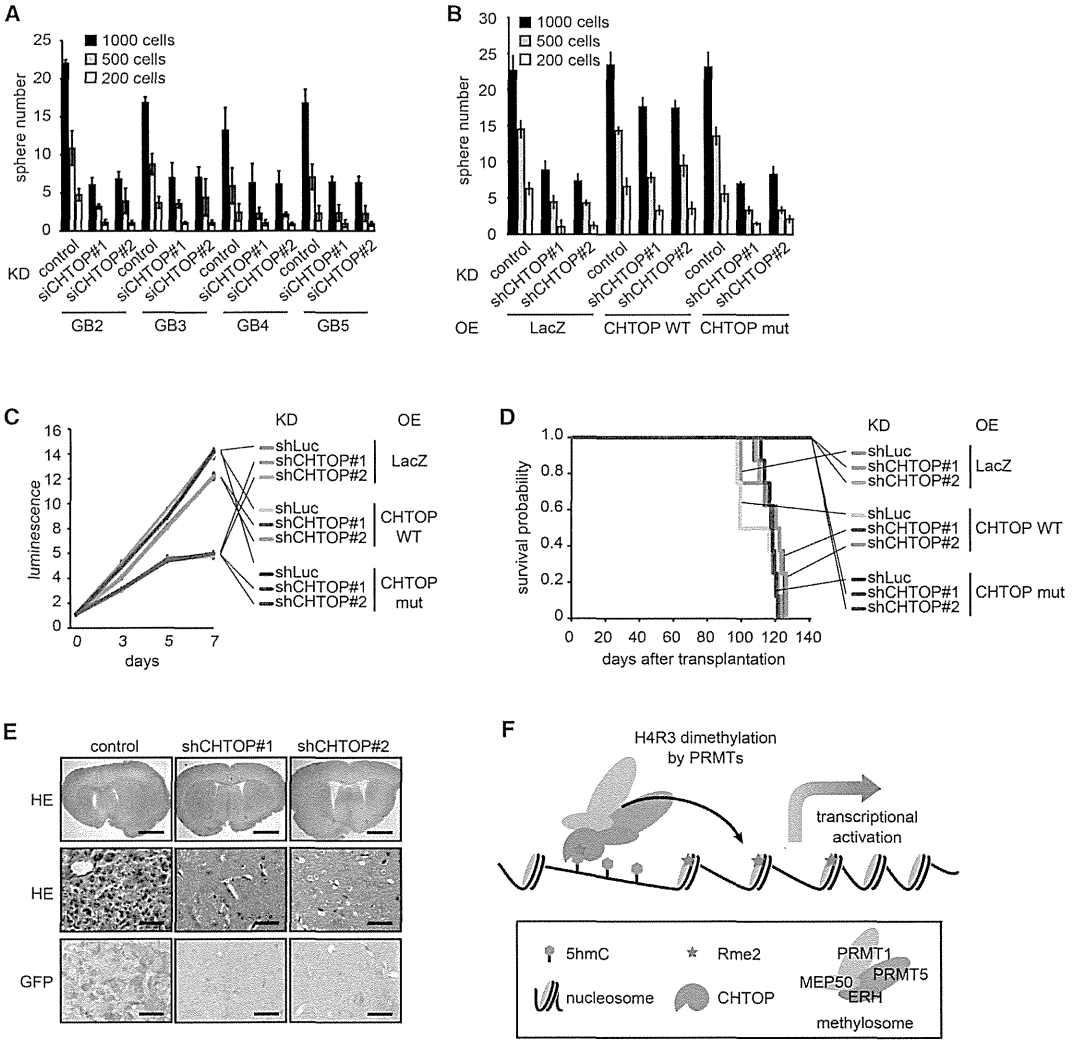

Figure 7. CHTOP Is Required for the Tumorigenicity of Glioblastoma Cells

(A) The number of spheres of glioblastoma cells transfected with siRNA targeting CHTOP. Data show the means ± SD of three independent experiments.

(B) The number of spheres of GB2 cells infected with a lentivirus expressing shRNA targeting CHTOP and/or a lentivirus expressing wild-type or mutant CHTOP. Data show the means ± SD of three independent experiments.

(C) Growth curves of GB2 cells infected with a lentivirus expressing shRNA targeting CHTOP and/or a lentivirus expressing wild-type or mutant CHTOP. Data show the means ± SD of three independent experiments.

(D) Kaplan-Meier survival curves of mice transplanted with 1.0×10^4 GB2 cells infected with a lentivirus expressing shRNA targeting CHTOP and/or a lentivirus expressing wild-type or mutant CHTOP.

(E) Histological examination of tumors developed in the mice in (D). At day 100, tissue sections were stained with HE or anti-GFP antibody. The scale bars represent 2 mm (upper panels) and 50 μm (lower panels).

(F) Schematic representation of 5hmC-mediated transcriptional activation. For details, see text.

See also Figure S6.

GB2~GB5 cells (Figures 7A and 7B) and GB2 cell proliferation (Figure 7C). These phenotypes were rescued by overexpression of wild-type CHTOP, but not by GAR mutant CHTOP. Mice receiving shCHTOP-expressing GB2 cells survived significantly longer than control mice (Figures 7D and 7E). Furthermore, we found that overexpression of CHTOP restored the tumorigenicity of shCHTOP-expressing GB2 cells (Figure 7D). These results suggest that 5hmC serves as a recruitment signal for the CHTOP-methylosome complex, which in turn methylates H4R3 and thereby activates the transcription of genes required for glioblastomagenesis (Figure 7F).

DISCUSSION

It is well known that glioblastomas contain genetic alterations in the p53, RB, and RTK pathways (Chen et al., 2012; Parsons

et al., 2008; Cancer Genome Atlas Research Network, 2008), as well as other genes, including the neurofibromatosis type 1 gene (Cancer Genome Atlas Research Network, 2008), the NF-κB inhibitor α gene (Bredel et al., 2011), and/or the IDH1 gene (Parsons et al., 2008). In the present study, we have shown that epigenetic alterations are also critical for the tumorigenicity of glioblastoma cells. We showed that proneural glioblastoma contains elevated levels of 5hmC and TET1 and that TET1-mediated production of 5hmC is required for glioblastomagenesis. We found that knockdown of TET1 in glioblastoma cells resulted in decreases in their proliferation, sphere formation, and tumorigenicity. Furthermore, we demonstrated that ectopic overexpression of wild-type, but not of a catalytically inactive mutant, TET1 restored the growth, sphere formation, and tumorigenicity, as well as 5hmC levels in glioblastoma cells in which TET1 had been knocked down.

Our results are in striking contrast to previous studies showing that 5hmC levels are markedly reduced in many tumor cells (Haffner et al., 2011; Kraus et al., 2012; Müller et al., 2012; Orr et al., 2012). This may be due to the differences in the culture conditions used and/or tumor subtypes. We cultured primary glioblastoma cells in serum-free conditions to retain their stem-cell-like properties and tumorigenicity. Indeed, our results showed that HeLa and U87MG cells cultured in the presence of serum contain extremely low levels of 5hmC.

Although most of previous studies did not consider subtypes of glioblastoma, Noushmehr et al. (2010) have reported that the IDH1 mutation is highly enriched in recurrent and secondary proneural glioblastoma and is strongly linked to the glioma-CpG island methylator phenotype (G-CIMP). Thus, secondary proneural glioblastomas are expected to have lower 5hmC levels. However, they have also reported that only a minor population of primary glioblastoma patients (<10%) display G-CIMP and IDH1 mutations. In this study, we focused on primary glioblastomas that can be cultured in serum-free media and found that most of the glioblastoma cell lines we established belong to the proneural subtype. Furthermore, we performed dot blot analysis of 5hmC using glioblastoma specimens of all subtypes and found that primary proneural glioblastomas that do not have an IDH1 mutation have markedly higher levels of 5hmC compared to other subtypes. We speculate that 5hmC may function differently at the molecular level in primary proneural glioblastoma compared to other subtypes of glioblastoma and other tumor cell types, and accordingly, 5hmC may recruit different molecules and elicit different downstream signals in proneural glioblastoma cells than it does in other tumor cells.

We have shown that 5hmC is not simply a demethylation intermediate but rather functions itself as an epigenetic mark modulating gene expression. Our results are consistent with previous findings showing that 5hmC is stably present in the genomes of ESCs and neuronal cells (Ficz et al., 2011; Guo et al., 2011; Hahn et al., 2013; Wu et al., 2011) and that enrichment of 5hmC is not necessarily associated with DNA demethylation (Hahn et al., 2013). Furthermore, Mbd3/NURD and MeCP2 have been reported to bind to both 5hmC and 5mC (Mellén et al., 2012; Yildirim et al., 2011). A systematic analysis of 5hmC-binding proteins using quantitative mass-spectrometry-based proteomics has identified a number of specific 5hmC-binding proteins (Spruijt et al., 2013). These reported results suggested that 5hmC, 5fC, and 5caC may recruit transcription regulators in certain cell types, as well as DNA repair proteins, which may also be involved in DNA demethylation. CHTOP was not identified in this latter study, presumably because this laboratory used mouse ESCs, mNPCs, and adult mouse brain tissue.

We found that TET1-mediated enrichment of 5hmC is critical for the expression of a number of cancer-related genes such as *EGFR*, *AKT3*, *CDK6*, *CCND2*, and *BRAF*. Furthermore, we found that CHTOP associated with 5hmC recruits the methylosome and that a component of the methylosome complex, PRMT1, methylates H4R3 and transactivates these genes. We investigated these genes because their products are key components of the RTK/RAS/PI(3)K- or the RB-signaling pathways and have been reported to be frequently altered in glioblastoma and play critical roles in glioblastomagenesis (Chen et al., 2012; Parsons et al., 2008; Cancer Genome Atlas Research Network, 2008). We would like to investigate whether hydroxymethylation of these five genes is necessary for the tumorigenicity of glioblastoma cells in future studies.

We found that TET1 knockdown in GB2 cells alters expression of many genes that do not have 5hmC peaks. It is possible that alterations in the expression of the genes that have 5hmC may affect that of other genes that do not have 5hmC. In addition, previous studies have shown that the TET family of proteins can interact with O-linked N-acetylglucosamine transferase (OGT) and function as a recruiter of OGT to chromatin (Chen et al., 2013; Deplus et al., 2013; Vella et al., 2013). We therefore speculate that TET1 has an important role that is independent of its catalytic activity.

Interestingly, we found that knockdown of CHTOP results in a reduction in global 5hmC levels in glioblastoma cells, whereas overexpression of CHTOP restores 5hmC levels. Thus, CHTOP may be required for maintaining 5hmC levels. For example, CHTOP may protect 5hmC from demethylation. Our results suggest that upregulation of CHTOP as well as TET1 may be responsible for the elevated levels of 5hmC observed in glioblastoma cells. We would like to investigate this issue in more detail in future studies. In addition, we found that hNPCs express somewhat lower levels of CHTOP than glioblastoma cells. It is therefore possible that reduced expression of CHTOP in hNPCs contributes, at least in part, to the poor expression of 5hmC, despite high TET1 expression in these cells.

Glioblastoma stem cells are subsets of glioblastoma cells that possess the capability of self-renewal and exhibit extensive tumorigenicity (Gilbertson and Rich, 2007; Lathia et al., 2011; Singh et al., 2004). Glioblastoma stem cells have been reported to be resistant to both chemotherapy and radiotherapy and thus are responsible for the poor prognosis of glioblastoma (Bao et al., 2006; Chen et al., 2012). In this study, we utilized glioblastoma cells cultured in serum-free medium, which enriches for glioblastoma stem cells (Lee et al., 2006). Thus, it is possible that 5hmC is critical for the tumorigenicity of glioblastoma stem cells. To test this possibility, we need to analyze the CD15- and/or CD133-positive stem cell population (Singh et al., 2004; Son et al., 2009). It also remains to be examined whether 5hmC is required specifically for glioblastoma stem cells or required for both glioblastoma stem and nonstem cells.

OPEN ACCESS
CellPress

In conclusion, we found that 5hmC recruits the CHTOP-methylosome complex, which methylates H4R3 and transactivates cancer-related genes. Of particular interest is the fact that knockdown of TET1 as well as CHTOP results in the strong suppression of glioblastoma cell tumorigenicity. We therefore speculate that TET1 could be a promising molecular target for glioblastoma therapy. Because TET1-deficient mice are viable and fertile (Dawlaty et al., 2011, 2013), compounds targeting TET1 would be expected to have few serious side effects.

EXPERIMENTAL PROCEDURES

Antibodies

Antibodies used in immunoblot, ChIP, and (h)MeDIP assays are listed in Table S4.

Cell Culture

Following informed consent, tumor samples classified as primary glioblastoma were obtained from patients undergoing surgical treatment at the University of Tokyo Hospital, as approved by the Institutional Review Board. Mouse experiments were also approved by the Institutional Review Board. Tumors were washed and mechanically and enzymatically dissociated into single cells. Tumor cells were cultured in Dulbecco's modified Eagle's medium (DMEM)/F12 (Life Technologies) containing B27 supplement minus vitamin A (Life Technologies), epidermal growth factor, and fibroblast growth factor 2 (20 ng/ml each; Wako Pure Chemicals Industries). Fetal and ESC-derived hNPCs were purchased from Lonza and Millipore, respectively, and cultured under the same conditions. HEK293FT, HeLa, and human glioblastoma U87MG cells were cultured in DMEM (Nissui) containing 10% fetal bovine serum. GB2 cells transfected with siRNA targeting TET1 or control were seeded into a 96-well plate at the indicated cell number. The number of spheres was counted after 7 days. Cell viability was measured by CellTiter-Glo (Promega) according to the manufacturer's instructions.

RNAi

For lentivirus production, the lentiviral vector CS-Rfa-CG harboring an shRNA driven by the H1 promoter was transfected with the packaging vectors pCAG-HIV-gp and pCMV-VSV-G-RSV-Rev into HEK293FT cells using Lipofectamine 2000 Transfection Reagent (Life Technologies). All plasmids were kindly provided by H. Miyoshi (RIKEN BioResource Center). Virus supernatants were purified by ultracentrifugation at 25,000 rpm at 4°C for 90 min (SW28 rotor; Beckman Coulter Genomics). The target sequences for shRNAs are as follows: shTET1 no.1: 5′-GCATATTCCTTTGAAATAA-3′; shTET1 no. 2: 5′-GAACTAAACAAGATTAAGT-3′; shCHTOP no. 1: 5′-CTAAATGAGCGCTTTA CTA-3′; shCHTOP no. 2: 5′-CCAAGATGTCTCTAAATGA-3′. The infection efficiency of the lentiviruses was more than 95%, as judged by GFP or Venus fluorescence. Transfection of Stealth siRNA duplexes targeting human TET1 (Life Technologies; catalog no. 10620318 and 10620319) or Silencer Select Pre-Designed siRNA targeting human CHTOP (Life Technologies; catalog no. s25092 and s25093) were performed using Lipofectamine RNAiMAX (Life Technologies) according to the manufacturer's instructions.

RNA Isolation and qRT-PCR

Total RNA was prepared by the NucleoSpin RNA Clean-up kit (Macherey-Nagel) and reverse transcribed with PrimeScript Reverse Transcriptase (TaKaRa). qPCR reactions were performed with Sybr Green I using a LightCycler480 (Roche Applied Science). The results were normalized with the detected values for TATA box-binding protein mRNA. Absolute mRNA levels of the TET family of genes were determined according to the standard curves generated by serial dilutions of plasmids containing TET1∼TET3. Primers used in qRT-PCR are shown in Table S5.

(h)MeDIP

Cells were digested with proteinase K and RNase A, and genomic DNA was purified by phenol/chloroform extraction. Purified genomic DNA was sonicated to 200–500 bp with a Handy Sonic (TOMY). (h)MeDIP was performed as described previously (Weber et al., 2005) with minor modifications. Briefly, 4 μg of fragmented genomic DNA was immunoprecipitated with 4 μl of polyclonal antibody against 5hmC (Active Motif) or 4 μg of monoclonal antibody against 5mC (Eurogentec) at 4°C overnight in a 500 μl of IP buffer (10 mM sodium phosphate [pH 7.0], 140 mM NaCl, and 0.05% Triton X-100). The mixture was incubated with 30 μl of Dynabeads Protein G at 4°C for 2 hr and washed three times with 1 ml of IP buffer. The beads were suspended in 20 μg of proteinase K and incubated at 55°C for at least 3 hr. Immunoprecipitated DNA was purified by phenol/chloroform extraction followed by isopropanol precipitation.

ACCESSION NUMBERS

Profiling and (h)MeDIP-seq data from this study are available from the Sequence Read Archive database (http://www.ncbi.nlm.nih.gov/sra) under the accession number SRP045590.

SUPPLEMENTAL INFORMATION

Supplemental Information includes Supplemental Experimental Procedures, six figures and five tables and can be found with this article online at http://dx.doi.org/10.1016/j.celrep.2014.08.071.

AUTHOR CONTRIBUTIONS

H.T. designed and performed most of the experiments. T. Sato performed dot blot analysis. R.K.-N. and Y.N.-N. established glioblastoma cell lines and discussed the results. K.M., Y.K., and K.S. performed sequence analysis and analyzed the bioinformatic data. H.O. and C.T. supervised the production of recombinant CHTOP. Y.M. performed immunohistochemical analysis of glioblastoma specimens. Y.S., Takeo Suzuki, Tsutomu Suzuki, H.K.-H., and M.O. performed mass spectrometric analysis. T.T., Y.I., A.M., and N.S. prepared glioblastoma specimens. H.T. and T.A. wrote the paper.

ACKNOWLEDGMENTS

This work was supported by Research Program of Innovative Cell Biology by Innovative Technology (Integrated Systems Analysis of Cellular Oncogenic Signaling Networks), Grants-in-Aid for Scientific Research on Innovative Areas (Integrative Research on Cancer Microenvironment Network), Project for Development of Innovative Research on Cancer Therapeutics, Takeda Science Foundation, and in part by Global COE Program (Integrative Life Science Based on the Study of Biosignaling Mechanisms), MEXT, Japan.

Received: April 5, 2014
Revised: July 29, 2014
Accepted: August 27, 2014
Published: October 2, 2014

REFERENCES

Bao, S., Wu, Q., McLendon, R.E., Hao, Y., Shi, Q., Hjelmeland, A.B., Dewhirst, M.W., Bigner, D.D., and Rich, J.N. (2006). Glioma stem cells promote radioresistance by preferential activation of the DNA damage response. Nature *444*, 756–760.

Baylin, S.B., and Jones, P.A. (2011). A decade of exploring the cancer epigenome - biological and translational implications. Nat. Rev. Cancer *11*, 726–734.

Bedford, M.T., and Clarke, S.G. (2009). Protein arginine methylation in mammals: who, what, and why. Mol. Cell *33*, 1–13.

Bird, A. (2001). Molecular biology. Methylation talk between histones and DNA. Science *294*, 2113–2115.

Bredel, M., Scholtens, D.M., Yadav, A.K., Alvarez, A.A., Renfrow, J.J., Chandler, J.P., Yu, I.L., Carro, M.S., Dai, F., Tagge, M.J., et al. (2011). NFKBIA deletion in glioblastomas. N. Engl. J. Med. *364*, 627–637.

Cancer Genome Atlas Research Network (2008). Comprehensive genomic characterization defines human glioblastoma genes and core pathways. Nature *455*, 1061–1068.

Chen, J., Li, Y., Yu, T.S., McKay, R.M., Burns, D.K., Kernie, S.G., and Parada, L.F. (2012). A restricted cell population propagates glioblastoma growth after chemotherapy. Nature *488*, 522–526.

Chen, Q., Chen, Y., Bian, C., Fujiki, R., and Yu, X. (2013). TET2 promotes histone O-GlcNAcylation during gene transcription. Nature *493*, 561–564.

Cimmino, L., Abdel-Wahab, O., Levine, R.L., and Aifantis, I. (2011). TET family proteins and their role in stem cell differentiation and transformation. Cell Stem Cell *9*, 193–204.

Dang, L., White, D.W., Gross, S., Bennett, B.D., Bittinger, M.A., Driggers, E.M., Fantin, V.R., Jang, H.G., Jin, S., Keenan, M.C., et al. (2009). Cancer-associated IDH1 mutations produce 2-hydroxyglutarate. Nature *462*, 739–744.

Dawlaty, M.M., Ganz, K., Powell, B.E., Hu, Y.C., Markoulaki, S., Cheng, A.W., Gao, Q., Kim, J., Choi, S.W., Page, D.C., and Jaenisch, R. (2011). Tet1 is dispensable for maintaining pluripotency and its loss is compatible with embryonic and postnatal development. Cell Stem Cell *9*, 166–175.

Dawlaty, M.M., Breiling, A., Le, T., Raddatz, G., Barrasa, M.I., Cheng, A.W., Gao, Q., Powell, B.E., Li, Z., Xu, M., et al. (2013). Combined deficiency of Tet1 and Tet2 causes epigenetic abnormalities but is compatible with postnatal development. Dev. Cell *24*, 310–323.

Delhommeau, F., Dupont, S., Della Valle, V., James, C., Trannoy, S., Massé, A., Kosmider, O., Le Couedic, J.P., Robert, F., Alberdi, A., et al. (2009). Mutation in TET2 in myeloid cancers. N. Engl. J. Med. *360*, 2289–2301.

Deplus, R., Delatte, B., Schwinn, M.K., Defrance, M., Méndez, J., Murphy, N., Dawson, M.A., Volkmar, M., Putmans, P., Calonne, E., et al. (2013). TET2 and TET3 regulate GlcNAcylation and H3K4 methylation through OGT and SET1/COMPASS. EMBO J. *32*, 645–655.

Ficz, G., Branco, M.R., Seisenberger, S., Santos, F., Krueger, F., Hore, T.A., Marques, C.J., Andrews, S., and Reik, W. (2011). Dynamic regulation of 5-hydroxymethylcytosine in mouse ES cells and during differentiation. Nature *473*, 398–402.

Figueroa, M.E., Abdel-Wahab, O., Lu, C., Ward, P.S., Patel, J., Shih, A., Li, Y., Bhagwat, N., Vasanthakumar, A., Fernandez, H.F., et al. (2010). Leukemic IDH1 and IDH2 mutations result in a hypermethylation phenotype, disrupt TET2 function, and impair hematopoietic differentiation. Cancer Cell *18*, 553–567.

Friesen, W.J., Paushkin, S., Wyce, A., Massenet, S., Pesiridis, G.S., Van Duyne, G., Rappsilber, J., Mann, M., and Dreyfuss, G. (2001). The methylosome, a 20S complex containing JBP1 and pICln, produces dimethylarginine-modified Sm proteins. Mol. Cell. Biol. *21*, 8289–8300.

Furnari, F.B., Fenton, T., Bachoo, R.M., Mukasa, A., Stommel, J.M., Stegh, A., Hahn, W.C., Ligon, K.L., Louis, D.N., Brennan, C., et al. (2007). Malignant astrocytic glioma: genetics, biology, and paths to treatment. Genes Dev. *21*, 2683–2710.

Gilbertson, R.J., and Rich, J.N. (2007). Making a tumour's bed: glioblastoma stem cells and the vascular niche. Nat. Rev. Cancer *7*, 733–736.

Goldberg, A.D., Allis, C.D., and Bernstein, E. (2007). Epigenetics: a landscape takes shape. Cell *128*, 635–638.

Guo, J.U., Su, Y., Zhong, C., Ming, G.L., and Song, H. (2011). Hydroxylation of 5-methylcytosine by TET1 promotes active DNA demethylation in the adult brain. Cell *145*, 423–434.

Haffner, M.C., Chaux, A., Meeker, A.K., Esopi, D.M., Gerber, J., Pellakuru, L.G., Toubaji, A., Argani, P., Iacobuzio-Donahue, C., Nelson, W.G., et al. (2011). Global 5-hydroxymethylcytosine content is significantly reduced in tissue stem/progenitor cell compartments and in human cancers. Oncotarget *2*, 627–637.

Hahn, M.A., Qiu, R., Wu, X., Li, A.X., Zhang, H., Wang, J., Jui, J., Jin, S.G., Jiang, Y., Pfeifer, G.P., and Lu, Q. (2013). Dynamics of 5-hydroxymethylcytosine and chromatin marks in mammalian neurogenesis. Cell Rep. *3*, 291–300.

He, Y.F., Li, B.Z., Li, Z., Liu, P., Wang, Y., Tang, Q., Ding, J., Jia, Y., Chen, Z., Li, L., et al. (2011). Tet-mediated formation of 5-carboxylcytosine and its excision by TDG in mammalian DNA. Science *333*, 1303–1307.

Hsu, C.H., Peng, K.L., Kang, M.L., Chen, Y.R., Yang, Y.C., Tsai, C.H., Chu, C.S., Jeng, Y.M., Chen, Y.T., Lin, F.M., et al. (2012). TET1 suppresses cancer invasion by activating the tissue inhibitors of metalloproteinases. Cell Rep. *2*, 568–579.

Huang, S., Litt, M., and Felsenfeld, G. (2005). Methylation of histone H4 by arginine methyltransferase PRMT1 is essential in vivo for many subsequent histone modifications. Genes Dev. *19*, 1885–1893.

Ito, S., Shen, L., Dai, Q., Wu, S.C., Collins, L.B., Swenberg, J.A., He, C., and Zhang, Y. (2011). Tet proteins can convert 5-methylcytosine to 5-formylcytosine and 5-carboxylcytosine. Science *333*, 1300–1303.

Jones, P.A. (2012). Functions of DNA methylation: islands, start sites, gene bodies and beyond. Nat. Rev. Genet. *13*, 484–492.

Koh, K.P., Yabuuchi, A., Rao, S., Huang, Y., Cunniff, K., Nardone, J., Laiho, A., Tahiliani, M., Sommer, C.A., Mostoslavsky, G., et al. (2011). Tet1 and Tet2 regulate 5-hydroxymethylcytosine production and cell lineage specification in mouse embryonic stem cells. Cell Stem Cell *8*, 200–213.

Koyama-Nasu, R., Nasu-Nishimura, Y., Todo, T., Ino, Y., Saito, N., Aburatani, H., Funato, K., Echizen, K., Sugano, H., Haruta, R., et al. (2013). The critical role of cyclin D2 in cell cycle progression and tumorigenicity of glioblastoma stem cells. Oncogene *32*, 3840–3845.

Kraus, T.F., Globisch, D., Wagner, M., Eigenbrod, S., Widmann, D., Münzel, M., Müller, M., Pfaffeneder, T., Hackner, B., Feiden, W., et al. (2012). Low values of 5-hydroxymethylcytosine (5hmC), the "sixth base," are associated with anaplasia in human brain tumors. Int. J. Cancer *131*, 1577–1590.

Lathia, J.D., Heddleston, J.M., Venere, M., and Rich, J.N. (2011). Deadly teamwork: neural cancer stem cells and the tumor microenvironment. Cell Stem Cell *8*, 482–485.

Lee, J., Kotliarova, S., Kotliarov, Y., Li, A., Su, Q., Donin, N.M., Pastorino, S., Purow, B.W., Christopher, N., Zhang, W., et al. (2006). Tumor stem cells derived from glioblastomas cultured in bFGF and EGF more closely mirror the phenotype and genotype of primary tumors than do serum-cultured cell lines. Cancer Cell *9*, 391–403.

Lian, C.G., Xu, Y., Ceol, C., Wu, F., Larson, A., Dresser, K., Xu, W., Tan, L., Hu, Y., Zhan, Q., et al. (2012). Loss of 5-hydroxymethylcytosine is an epigenetic hallmark of melanoma. Cell *150*, 1135–1146.

Lottaz, C., Beier, D., Meyer, K., Kumar, P., Hermann, A., Schwarz, J., Junker, M., Oefner, P.J., Bogdahn, U., Wischhusen, J., et al. (2010). Transcriptional profiles of CD133+ and CD133- glioblastoma-derived cancer stem cell lines suggest different cells of origin. Cancer Res. *70*, 2030–2040.

Martin, C., and Zhang, Y. (2005). The diverse functions of histone lysine methylation. Nat. Rev. Mol. Cell Biol. *6*, 838–849.

Mellén, M., Ayata, P., Dewell, S., Kriaucionis, S., and Heintz, N. (2012). MeCP2 binds to 5hmC enriched within active genes and accessible chromatin in the nervous system. Cell *151*, 1417–1430.

Meshorer, E., Yellajoshula, D., George, E., Scambler, P.J., Brown, D.T., and Misteli, T. (2006). Hyperdynamic plasticity of chromatin proteins in pluripotent embryonic stem cells. Dev. Cell *10*, 105–116.

Müller, T., Gessi, M., Waha, A., Isselstein, L.J., Luxen, D., Freihoff, D., Freihoff, J., Becker, A., Simon, M., Hammes, J., et al. (2012). Nuclear exclusion of TET1 is associated with loss of 5-hydroxymethylcytosine in IDH1 wild-type gliomas. Am. J. Pathol. *181*, 675–683.

Noushmehr, H., Weisenberger, D.J., Diefes, K., Phillips, H.S., Pujara, K., Berman, B.P., Pan, F., Pelloski, C.E., Sulman, E.P., Bhat, K.P., et al. (2010). Identification of a CpG island methylator phenotype that defines a distinct subgroup of glioma. Cancer Cell *17*, 510–522.

Ono, R., Taki, T., Taketani, T., Taniwaki, M., Kobayashi, H., and Hayashi, Y. (2002). LCX, leukemia-associated protein with a CXXC domain, is fused to MLL in acute myeloid leukemia with trilineage dysplasia having t(10;11)(q22;q23). Cancer Res. *62*, 4075–4080.

Orr, B.A., Haffner, M.C., Nelson, W.G., Yegnasubramanian, S., and Eberhart, C.G. (2012). Decreased 5-hydroxymethylcytosine is associated with neural progenitor phenotype in normal brain and shorter survival in malignant glioma. PLoS ONE *7*, e41036.

Parsons, D.W., Jones, S., Zhang, X., Lin, J.C., Leary, R.J., Angenendt, P., Mankoo, P., Carter, H., Siu, I.M., Gallia, G.L., et al. (2008). An integrated genomic analysis of human glioblastoma multiforme. Science *321*, 1807–1812.

Rajyaguru, P., and Parker, R. (2012). RGG motif proteins: modulators of mRNA functional states. Cell Cycle *11*, 2594–2599.

Sasaki, H., and Matsui, Y. (2008). Epigenetic events in mammalian germ-cell development: reprogramming and beyond. Nat. Rev. Genet. *9*, 129–140.

Shen, L., Song, C.X., He, C., and Zhang, Y. (2014). Mechanism and function of oxidative reversal of DNA and RNA methylation. Annu. Rev. Biochem. *83*, 585–614.

Singh, S.K., Hawkins, C., Clarke, I.D., Squire, J.A., Bayani, J., Hide, T., Henkelman, R.M., Cusimano, M.D., and Dirks, P.B. (2004). Identification of human brain tumour initiating cells. Nature *432*, 396–401.

Son, M.J., Woolard, K., Nam, D.H., Lee, J., and Fine, H.A. (2009). SSEA-1 is an enrichment marker for tumor-initiating cells in human glioblastoma. Cell Stem Cell *4*, 440–452.

Spruijt, C.G., Gnerlich, F., Smits, A.H., Pfaffeneder, T., Jansen, P.W., Bauer, C., Münzel, M., Wagner, M., Müller, M., Khan, F., et al. (2013). Dynamic readers for 5-(hydroxy)methylcytosine and its oxidized derivatives. Cell *152*, 1146–1159.

Stupp, R., Mason, W.P., van den Bent, M.J., Weller, M., Fisher, B., Taphoorn, M.J., Belanger, K., Brandes, A.A., Marosi, C., Bogdahn, U., et al.; European Organisation for Research and Treatment of Cancer Brain Tumor and Radiotherapy Groups; National Cancer Institute of Canada Clinical Trials Group (2005). Radiotherapy plus concomitant and adjuvant temozolomide for glioblastoma. N. Engl. J. Med. *352*, 987–996.

Tahiliani, M., Koh, K.P., Shen, Y., Pastor, W.A., Bandukwala, H., Brudno, Y., Agarwal, S., Iyer, L.M., Liu, D.R., Aravind, L., and Rao, A. (2009). Conversion of 5-methylcytosine to 5-hydroxymethylcytosine in mammalian DNA by MLL partner TET1. Science *324*, 930–935.

van Dijk, T.B., Gillemans, N., Stein, C., Fanis, P., Demmers, J., van de Corput, M., Essers, J., Grosveld, F., Bauer, U.M., and Philipsen, S. (2010). Friend of Prmt1, a novel chromatin target of protein arginine methyltransferases. Mol. Cell. Biol. *30*, 260–272.

Vella, P., Scelfo, A., Jammula, S., Chiacchiera, F., Williams, K., Cuomo, A., Roberto, A., Christensen, J., Bonaldi, T., Helin, K., and Pasini, D. (2013). Tet proteins connect the O-linked N-acetylglucosamine transferase Ogt to chromatin in embryonic stem cells. Mol. Cell *49*, 645–656.

Wang, H., Huang, Z.Q., Xia, L., Feng, Q., Erdjument-Bromage, H., Strahl, B.D., Briggs, S.D., Allis, C.D., Wong, J., Tempst, P., and Zhang, Y. (2001). Methylation of histone H4 at arginine 3 facilitating transcriptional activation by nuclear hormone receptor. Science *293*, 853–857.

Ward, P.S., Patel, J., Wise, D.R., Abdel-Wahab, O., Bennett, B.D., Coller, H.A., Cross, J.R., Fantin, V.R., Hedvat, C.V., Perl, A.E., et al. (2010). The common feature of leukemia-associated IDH1 and IDH2 mutations is a neomorphic enzyme activity converting alpha-ketoglutarate to 2-hydroxyglutarate. Cancer Cell *17*, 225–234.

Weber, M., Davies, J.J., Wittig, D., Oakeley, E.J., Haase, M., Lam, W.L., and Schübeler, D. (2005). Chromosome-wide and promoter-specific analyses identify sites of differential DNA methylation in normal and transformed human cells. Nat. Genet. *37*, 853–862.

Wu, H., and Zhang, Y. (2014). Reversing DNA methylation: mechanisms, genomics, and biological functions. Cell *156*, 45–68.

Wu, H., D'Alessio, A.C., Ito, S., Wang, Z., Cui, K., Zhao, K., Sun, Y.E., and Zhang, Y. (2011). Genome-wide analysis of 5-hydroxymethylcytosine distribution reveals its dual function in transcriptional regulation in mouse embryonic stem cells. Genes Dev. *25*, 679–684.

Xu, W., Yang, H., Liu, Y., Yang, Y., Wang, P., Kim, S.H., Ito, S., Yang, C., Wang, P., Xiao, M.T., et al. (2011). Oncometabolite 2-hydroxyglutarate is a competitive inhibitor of α-ketoglutarate-dependent dioxygenases. Cancer Cell *19*, 17–30.

Yildirim, O., Li, R., Hung, J.H., Chen, P.B., Dong, X., Ee, L.S., Weng, Z., Rando, O.J., and Fazzio, T.G. (2011). Mbd3/NURD complex regulates expression of 5-hydroxymethylcytosine marked genes in embryonic stem cells. Cell *147*, 1498–1510.

Zullo, A.J., Michaud, M., Zhang, W., and Grusby, M.J. (2009). Identification of the small protein rich in arginine and glycine (SRAG): a newly identified nucleolar protein that can regulate cell proliferation. J. Biol. Chem. *284*, 12504–12511.

ELSEVIER

CrossMark

Experimental Hematology

Experimental Hematology 2014;42:816–825

Generation of induced pluripotent stem cells derived from primary and secondary myelofibrosis patient samples

Masataka Hosoi[a,b], Keiki Kumano[a,b], Kazuki Taoka[a,b], Shunya Arai[a,b], Keisuke Kataoka[a,b], Koki Ueda[a,b], Yasuhiko Kamikubo[a,b], Naoya Takayama[c], Makoto Otsu[d], Koji Eto[c], Hiromitsu Nakauchi[d], and Mineo Kurokawa[a,b]

[a]*Department of Hematology and Oncology, Graduate School of Medicine, University of Tokyo, Tokyo, Japan;* [b]*CREST, Japan Science and Technology Agency (JST), Tokyo, Japan;* [c]*Center for iPS Cell Research and Application, Kyoto University, Kyoto, Japan;* [d]*Division of Stem Cell Therapy, Center for Stem Cell Biology and Regenerative Medicine, Institute of Medical Science, University of Tokyo, Tokyo, Japan*

(Received 21 June 2013; revised 23 February 2014; accepted 3 March 2014)

Induced pluripotent stem cells (iPS) derived from disease cells are expected to provide a new experimental material, especially for diseases from which samples are difficult to obtain. In this study, we generated iPS from samples from patients with primary and secondary myelofibrosis. The primary myelofibrosis cells had chromosome 13q deletions, and the secondary myelofibrosis (SMF) cells had JAK2V617F mutations. The myelofibrosis patient cell-derived iPS (MF-iPS) were confirmed as possessing these parental disease-specific genomic markers. The capacity to form three germ layers was confirmed by teratoma assay. By co-culture with specific feeder cells and cytokines, MF-iPS can re-differentiate into blood progenitor cells and finally into megakaryocytes. We found that mRNA levels of interleukin-8, one of the candidate cytokines related to the pathogenesis of myelofibrosis, was elevated predominantly in megakaryocytes derived from MF-iPS. Because megakaryocytes from myelofibrosis clones are considered to produce critical mediators to proliferate fibroblasts in the bone marrow and iPS can provide differentiated cells abundantly, the disease-specific iPS we established should be a good research tool for this intractable disease. © **2014 ISEH - International Society for Experimental Hematology. Published by Elsevier Inc.**

Generation of induced pluripotent stem cells (iPS) from various types of human somatic cells provided promising views for new medical science [1]. After this breakthrough, disease modeling with the use of iPS technology attracted much attention, because iPS technology could provide human disease cell resources and new experimental opportunities that were hardly obtainable in the past [2].

Myelofibrosis is a pre-leukemic neoplastic disease with a generally poor prognosis, although the patients follow a diverse clinical course because of the pathophysiologic heterogeneity of this disease. Indeed, the median life expectancy of myelofibrosis patients is estimated to range from 27 to 135 months depending on the risk group [3]. Although a new therapeutic strategy targeting JAK2 had been tested, its curative effect has been found weaker than expected, compared with the tyrosine kinase inhibitors in practical use for chronic myeloid leukemia patients [4]. Cure is still limited to allogeneic hematopoietic stem cell transplantation, which, however, is associated with a high risk of treatment-related mortality and morbidity and, therefore, is indicated only for young patients without problematic complications [5–8]. Clearly, further investigations are needed to develop novel targeted therapies for myelofibrosis.

The mediators of stimulation of fibroblast proliferation derived from myeloproliferative neoplasms were thought to be cytokines, including basic fibroblast growth factor, platelet-derived growth factor (PDGF) and transforming growth factor β (TGF-β) [9,10]. Other candidate mediators recently reported as related to symptoms of myelofibrosis include hepatocyte growth factor, monokine induced by γ interferon, interleukin (IL)-1 receptor antagonist associated with marked splenomegaly, and IL-8 associated with severe constitutional symptoms [11]. Megakaryocytes, as well as monocytes, derived from neoplasms contain these cytokines and, thus, are one of the suspected main feeders of the responsible mediators [12–14]. However, because of the bone marrow fibrosis characteristic of myelofibrosis,

Offprint requests to: Mineo Kurokawa, Department of Hematology & Oncology, Graduate School of Medicine, University of Tokyo, 7-3-1 Hongo, Bunkyo-ku, Tokyo 113-8655, Japan; E-mail: kurokawa-tky@umin.ac.jp

0301-472X/$ - see front matter. Copyright © 2014 ISEH - International Society for Experimental Hematology. Published by Elsevier Inc.
http://dx.doi.org/10.1016/j.exphem.2014.03.010

primary sufficient hematopoietic samples such as megakaryocytes are hard to obtain. Currently, a certain amount of megakaryocytes from myelofibrosis patients can be obtained only by differentiation of peripheral blood progenitor cells or by the surgical resection of extramedullary lesions [15,16]

In this study, we generated iPS from primary samples of a patient with primary and a patient with secondary myelofibrosis and re-differentiated them into hematopoietic cells including megakaryocytes. These iPS would be a new material for investigating pathogenic mechanisms of myelofibrosis.

Methods

Cells and cell culture

All studies using human cells were reviewed and approved by the institutional review boards of the University of Tokyo. After written informed consent was obtained, bone marrow cells were collected from a patient with primary myelofibrosis and peripheral blood cells from a patient with secondary myelofibrosis. Mobilized peripheral blood cells of a healthy donor for peripheral blood stem cell transplantation were also obtained after informed consent. The characteristics of the patients are listed in Table 1. Both patients were in the intermediate-2 risk group with the same two risk factors—constitutional symptoms and blood blasts >1%—according to the prognostic scoring system of the International Working Group of Myelofibrosis Research and Treatment [3]. We then isolated mononuclear cells from the samples by centrifugation using Lymphoprep (Axis-Shield, Oslo, Norway). We concentrated $CD34^+$ cells using an immunomagnetic separation technique with AUTO MACS (Milteny Biotec, Bergisch-Gladbach, Germany). These cells were cultured with α-MEM containing 20% fetal calf serum, penicillin, streptomycin, 2 mM 2-mercaptoethanol supplemented with 100 ng/mL recombinant human stem cell factor (SCF, Wako Pure Chemical, Osaka, Japan), 10 ng/mL recombinant human thrombopoietin (Kyowa Hakko Kirin, Tokyo, Japan), 100 ng/mL recombinant human FMS-like tyrosine kinase 3 ligand (FL3L, Wako), 10 ng/mL recombinant human IL-3 (Wako), 100 ng/mL recombinant human IL-6 (Wako). Myelofibrosis patient cell-derived iPS (MF-iPS) were maintained in DMEM-F12 medium (Invitrogen, Life Technologies, Carlsbad, CA, USA) supplemented with 20% KnockOut Serum Replacement (KSR, Invitrogen), 0.1 mM 2-mercaptoethanol (Sigma–Aldrich, St. Louis, MO, USA), MEM non-essential amino acids (Invitrogen), penicillin–streptomycin–glutamine (Sigma–Aldrich), and 5 ng/mL recombinant human basic fibroblast growth factor (Peprotech, Rocky Hill, NJ, USA) on mitomycin C (Wako)-treated mouse embryo fibroblast feeder cells.

Table 1. Characteristics of patients

Feature	Secondary myelofibrosis	Primary myelofibrosis
Specific marker	JAK2 V617F mutation	13q deletion
Source of material	Peripheral blood cells	Bone marrow cells
Age	31 y	54 y
Sex	Female	Female
Constitutional symptoms	Yes	Yes
Palpable splenomegaly	Yes	Yes
Palpable hepatomegaly	Yes	Yes
Hemoglobin	13.1 g/dL	10.3 g/dL
White blood cell count	24.1 × 10^9/L	9.9 × 10^9/L
Platelets	481 × 10^9/L	106 × 10^9/L
Blood blasts	1.0%	1.0%

Mouse C3H10T1/2 cells were purchased from Riken Bio-Resource Center (Tsukuba, Japan) and cultured as previously described.

All cell culture procedures were performed in a humidified 37°C, 5% CO_2 environment.

Production of VSV-G pseudotyped retrovirus for reprogramming

The pMX vectors encoding OCT3/4, SOX2, KLF4 and c-MYC and highly concentrated vesicular stomatitis virus G glycoprotein (VSV-G) pseudotyped retroviral supernatants were prepared as reported previously [2]. With 293GPG cells, a kind gift from Dr. R. C. Mulligan (Children's Hospital Boston, Harvard Medical School, Boston, MA, USA), stable cell lines producing VSV-G pseudotyped retroviral particles containing either the OCT3/4, SOX2, KLF4, or c-MYC gene were established. We centrifuged these for 16 hours at 6000*g* and concentrated the viral supernatant by resuspension in Iscove's modified Dulbecco's medium.

Generation of iPS from primary patient samples

Fibronectin fragment CH296 (RetroNectin, Takara-Bio, Otsu, Japan)-coated plates and virus-bound plates were prepared without centrifugation according to the manufacturer's recommendation. Briefly, the wells were coated with 20 μg/mL RetroNectin and incubated overnight at 4°C. Then, the remaining free sites were blocked with 2% bovine serum albumin for 30 min at room temperature. After removal of bovine serum albumin solution and a phosphate-buffered saline wash, the well was filled with retroviral supernatants and incubated for 4 hours at 37°C. After the viral solution was removed, 1 × 10^5 $CD34^+$ concentrated patient cells, after stimulation with cytokines as mentioned above, were placed in each well, and the wells were filled with the stimulation culture medium supplemented with cytokines mentioned above. After 24 and 48 hours, viral supernatants were added to the culture medium. After the third infection, we harvested the cells by pipetting and seeded them on mitomycin C-treated mouse embryo fibroblast cells with fresh medium containing half the cytokines for the next 2 days. On day 5, we replaced the medium with the human embryonic stem medium described above containing 0.5 mM valproic acid (Sigma–Aldrich). The medium was changed every other day. After 14 to 21 days, colonies appeared. Morphologically determined human embryonic stem cell-like colonies were picked up and colony-derived cells were seeded separately on new mouse embryo fibroblast feeder cells as single clone-derived iPS should be established. Clones that expanded were used for further analyses.

Fluorescence immunostaining assay

Myelofibrosis iPS were fixed with 3.8% formaldehyde in phosphate-buffered saline and then blocked with 1% bovine serum albumin (Sigma-Aldrich). The antigens were labeled overnight with 1% each of anti-human SSEA-4 conjugated with Alexa480 antibody and anti-human TRA-1-60 conjugated with Alexa555

antibody. After counterstaining with 4-6-diamidino-2-phenylindole (DAPI), cells were observed with a FLUOVIEW FV10i (Olympus, Tokyo, Japan).

Semi-quantitative reverse transcription polymerase chain reaction

Total RNA was purified with the RNeasy Mini Kit (Qiagen, Hilden, Germany) or NucleoSpin RNA II (Macherey-Nagel, Düren, Germany) and used for reverse transcription with SuperScript III (Life Technologies) and random hexamer primer or PrimeScript RT Master Mix (Takara-Bio), according to the manufacturer's instructions. Primer sequences used to detect endogenous or exogenous expression of the stem cell genes were as described previously [1]. Primers for the GAPDH gene were (forward) ACCA CAGTCCATGCCATCAC and (reverse) TCCACCACCCTGTTG CTGTA.

Teratoma formation assay

Induced pluripotent stem cells grown confluently in a 6-cm dish were suspended in 40 μL phosphate-buffered saline containing 10 μM Y27632 (Wako), a ROCK-specific inhibitor added to preserve the viability of dissociated iPS. The cell suspension was injected into both testes of 8-week-old non-obese diabetic/severe combined immunodeficient mice. Ten weeks after injection, the developed tumors were harvested and fixed with 3.8% formaldehyde, embedded in paraffin, and stained with hematoxylin and eosin for histologic analysis.

Bisulfite assay

One microgram of genomic DNA was converted with the EpiTect Bisulfite Kit (Qiagen) according to the manufacturer's recommendations. The promoter region of the NANOG gene of treated DNA was amplified by polymerase chain reaction (PCR) with previously reported primers [1]. The PCR products were subcloned with the TA PCR Cloning Kit (DynaExpress, Tokyo, Japan). Ten clones from each sample were checked by sequencing with M13 universal primers.

Allele-specific PCR and sequence analyses of JAK2 gene

Polymerase chain reaction to detect the JAK2V617F allele or wild-type JAK2 allele of genomic DNA was performed using the following primer combinations: (forward JAK2V617F) AG CATTTGGTTTTAAATTATGGAGTATATT; (forward JAK2 wild type) AGCATTTGGTTTTAAATTATGGAGTATATG; reverse (both) CAAAAACAGATGCTCTGAGAAAGG. For sequence analysis, the following primers were used: forward primer for amplification of genomic DNA (JAK2 seq-FW1), ATCTATGT CATGCTGAAAGTAGGAGAAAG; reverse primer for amplification of genomic DNA (JAK2 seq-RV1), CTGAATAGTCCTA CAGTGTTTTCAGTTTCA; forward primer for sequence reaction (JAK2 seq-FW2), TTCCTTAGTCTTTCTTTGAAGC.

Fluorescence in situ hybridization

Primary myelofibrosis iPS were exposed to trypsin-EDTA and suspended to single cells by pipetting. After fixation, in situ hybridization was performed using Vysis LSI D13S319 (13q14.3) Probe (Abbott Laboratories, Abbot Park, IL, USA).

Karyotype analysis

Karyotype was determined by the G-band method (Nihon Gene Research Laboratories, Sendai, Japan).

Generation of hematopoietic progenitor cells from iPS

For differentiation of MF-iPS into hematopoietic cells, we adopted the protocol previously described [17,18]. Briefly, roughly broken iPS clumps (about 100 cells per clump; broken by pipetting, after normal dissociation with 0.25% trypsin, 1 mM $CaCl_2$, and 20% KnockOut Serum Replacement in phosphate-buffered saline) were disseminated on mitomycin C-treated 10T1/2 feeder cells with Iscove's modified Dulbecco medium containing 15% fetal calf serum (Life Technologies), 1% 100 × ITS Liquid Media Supplement (Sigma–Aldrich), 1% 100 × penicillin–streptomycin–glutamine (Life Technologies), 0.45 mM monothioglycerol (Sigma–Aldrich), 50 μg/mL ascorbic acid (Sigma–Aldrich) supplemented with 20 ng/mL recombinant human vascular endothelial growth factor A (R&D Systems, Minneapolis, MN, USA). The medium was replaced on days 3, 6, 9, 11, and 13. Cells in the "iPS sac" structure were harvested by pipetting and passed through a 40-μm cell strainer (BD Biosciences, Franklin Lakes, NJ, USA).

Methylcellulose colony assay

Sorted CD34 $^{+}$ 43^{+} progenitor cells (2400 cells) in methylcellulose H4434 Classic medium (Stemcell Technologies, Vancouver, BC, Canada) were plated in 35-mm petri dishes. The number of colonies was scored after 14 days of culture.

Lineage-specific differentiation of iPS-derived progenitors

For erythroid lineage differentiation, sorted CD34^{+}43^{+} progenitor cells were plated in round-bottom 96-well plates filled with the differentiation medium described above supplemented with 50 ng/mL stem cell factor, 3 IU/mL recombinant human erythropoietin (Kyowa Hakko Kirin), and 10 ng/mL IL-3. On days 3, 6, 9, and 12, half of the medium was replaced with fresh medium containing twice the concentrations listed above. On day 14, cells were harvested and analyzed. For myeloid lineage differentiation, sorted CD34 $^{+}$ 43^{+} progenitor cells were plated in six-well plates filled with α-MEM containing 20% fetal calf serum, penicillin, streptomycin, and 2 mM 2-mercaptoethanol supplemented with 100 ng/mL recombinant human stem cell factor, 10 ng/mL recombinant human thrombopoietin, 100 ng/mL recombinant human FL3L, 10 ng/mL recombinant human IL-3, and 100 ng/mL recombinant human IL-6. After a week of culture, cells were harvested and analyzed.

Differentiation of iPS-derived progenitors into megakaryocytes

To differentiate generated progenitor cells into megakaryocytes, we adopted the protocol previously described with a minor modification [17,18]. Sorted CD34^{+}43^{+} cells were plated on mitomycin C-treated fresh 10T1/2 cells. The medium used was Iscove's modified Dulbecco medium containing 15% fetal calf serum, 1% 100 × ITS, 1% penicillin–streptomycin–glutamine, 0.45 mM monothioglycerol (Sigma-Aldrich), and 50 μg/mL ascorbic acid supplemented with 25 ng/mL rHuMGDF (Kyowa Hakko Kirin), stem cell factor and heparin. On days 3 and 6, half of the medium was replaced with fresh medium containing twice the concentrations listed above.

Flow cytometry and morphology analysis

The following antibodies were used for fluorescence-activated cell sorting analysis and immunocytochemistry: anti-human CD34 APC conjugated (Beckman Coulter, Brea, CA, USA), anti-human CD43 PE conjugated (Beckman Coulter), anti-human

CD41a APC conjugated (BD Biosciences), and anti-human CD42b PE conjugated (Beckman Coulter). Cells were analyzed and sorted with a FACSAria (BD Biosciences), and cell morphology was observed after Wright–Giemsa staining.

DNA content assay

Sorted $CD41a^{+}42b^{+}$ megakaryocytes were incubated in staining medium for more than 30 min room temperature and used for fluorescence-activated cell sorting analysis. The staining medium contained 0.1 mg/mL propidium iodine (Sigma–Aldrich), 0.1% Triton X-100 (Sigma–Aldrich), 0.1% trisodium citrate dihydrate (Wako), and 50 μg/mL ribonuclease A (Nippon Gene, Tokyo, Japan).

Real-time reverse transcription PCR

Total RNA of sorted $CD41a^{+}42b^{+}$ megakaryocytes was extracted using the NucleoSpin RNA II (Macherey-Nagel), and cDNA was prepared with PrimeScript RT Master Mix (Takara-Bio). Real-time reverse transcription PCR was performed using a LightCycler 480 Real-Time PCR System and Light Cycler 2.0 instrument (Roche, Basel, Switzerland). cDNA was amplified using Thunderbird SYBR qPCR Mix (Toyobo, Osaka, Japan). The expression levels were normalized by those of 18S ribosomal RNA. The primer pairs used were as follows: forward primer for IL-8 (GenBank Accession No. NM_000584), TGAGAGTGATTGA GAGTGGACCA; reverse primer for IL-8, TCAGCCCTCTT CAAAAACTTCTCC; forward primer for PDGF alpha (GenBank accession number X06374) (PDGFa-FW), GCTGCT GCAACACGAGCAGT; reverse primer for PDGF-α, CCGGATT-CAGGCTTGTGGTC; forward primer for TGF-β1 (GenBank Accession No. NM_000660), TGAACCGGCCTTTCCTGCTT CTCATG; reverse primer for TGF-β1, GCGGAAGTCAATGTA CAGCTGCCGC; forward primer for 18S rRNA (GenBank Accession No. M10098), CAGCCACCCGAGATTGAGCA; reverse primer for 18S rRNA, TAGTAGCGACGGGCGGTGTG.

Statistical analyses

Statistical analyses were performed with the t test. A p value <0.05 was considered to indicate significance.

Results

Generation of iPS from primary and secondary myelofibrosis patient samples

$CD34^{+}$ cells were isolated from bone marrow or peripheral blood mononuclear cells of patients with primary and secondary myelofibrosis. We cultured these samples for 2 days with stimulating cytokines and transduced them with vesicular stomatitis virus G glycoprotein pseudotyped retroviruses containing OCT3/4, SOX2, KLF4, and c-MYC. Two days after transduction, we reseeded cells onto mouse embryo fibroblast feeder cells and continued culture for another 2 days. We then replaced all of the medium with the medium for human embryo stem cells containing 5 ng/mL basic fibroblast growth factor. Valproic acid, a histone deacetylase inhibitor, was added to the medium, to improve efficiency (Fig. 1). After about 3 weeks of culture, iPS colonies derived from primary and secondary myelofibrosis patients (MF-iPS) were established. The ratio of generated iPS colony number to that of applied cells was 0.0017% for the samples from the peripheral blood of the patient with SMF and 0.00075% for those from the bone marrow of the patient with primary myelofibrosis. The MF-iPS were morphologically similar to iPS derived from normal human cells (Fig. 2A). MF-iPS expressed SSEA-4 and TRA-1-60 pluripotency marker antigens (Fig. 2B) and, endogenously, the embryonic stem cell-related transcription factors OCT3/4, SOX2, c-MYC, and NANOG (Fig. 2C). Most of the virally delivered exogenous genes in MF-iPS were substantially silenced, except for a relatively high residual expression of OCT3/4 in a primary MF-iPS line (PMF-iPS) and KLF4 in a SMF-iPS line (Fig. 2D). Both primary and secondary MF-iPS could develop teratoma with three germ layers confirmed by histologic analyses (Fig. 2E). The undifferentiated status of secondary MF-iPS was also confirmed by analyses of the demethylated status of the NANOG promoter CpG island (Fig. 2F).

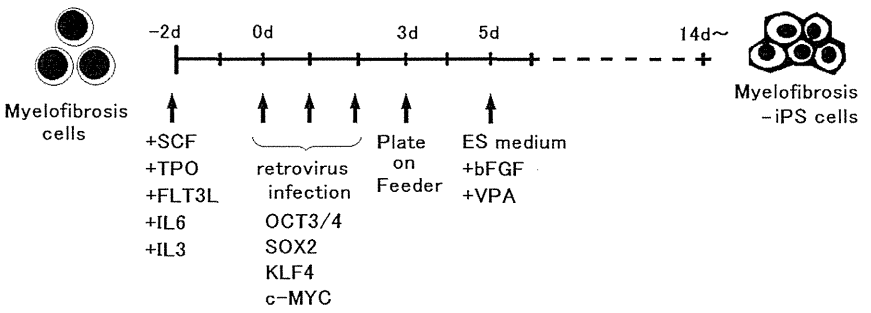

Figure 1. Experimental scheme for generating induced pluripotent stem cells from myelofibrosis patient samples. Yamanaka four factors was introduced to proliferation stimulated samples by retroviral vectors. Valproic acid was used to improve efficiency. bFGF = basic fibroblast growth factor, ES = embryonic stem cell culture medium, FLT3L = FMS-like tyrosine kinase 3 ligand, IL = interleukin, iPS = induced pluripotent stem cells, SCF = stem cell factor, TPO = thrombopoietin, VPA = valproic acid.

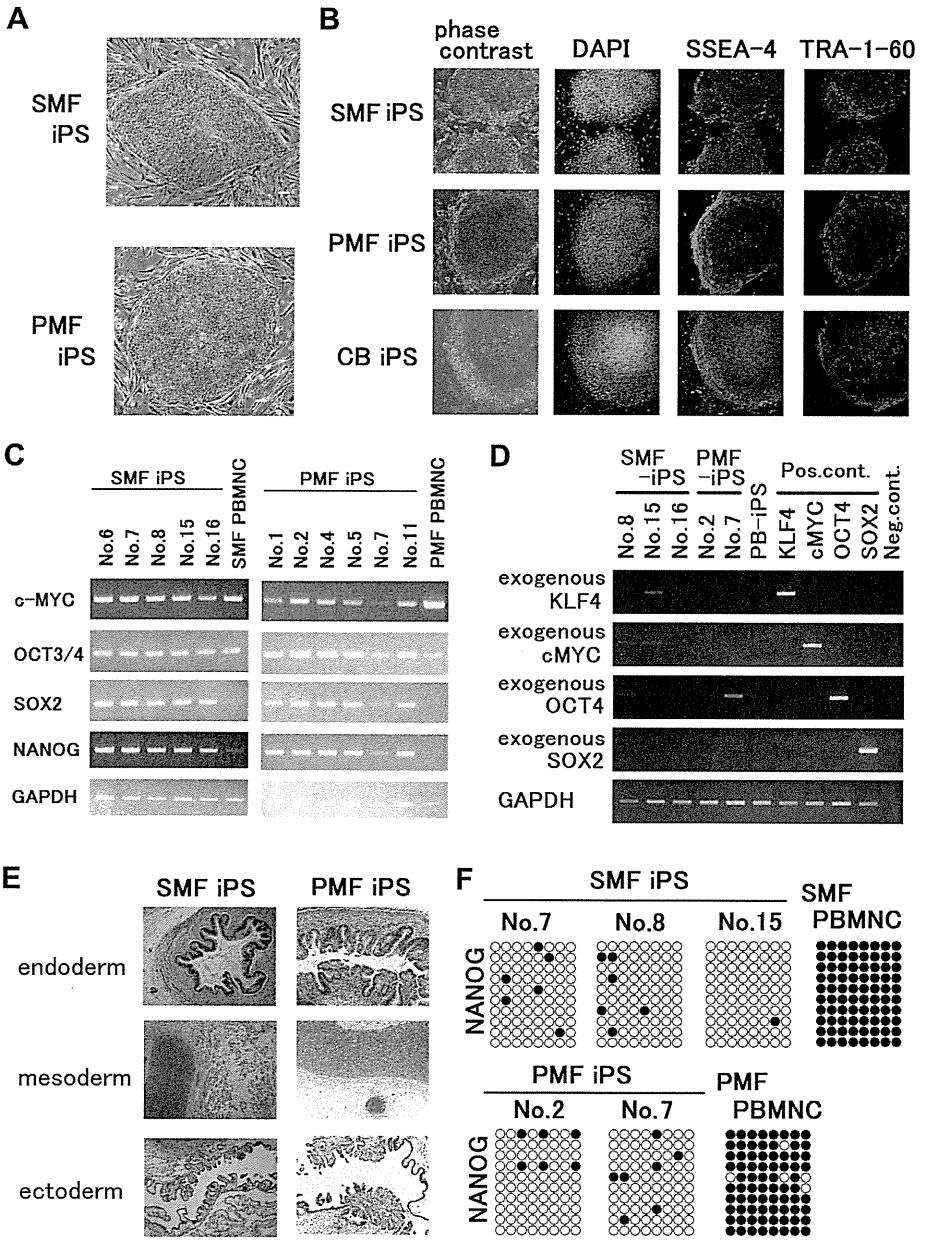

Figure 2. Pluripotency confirmation of myelofibrosis patient-derived induced pluripotent stem cells (iPS). (**A**) Morphology of myelofibrosis patient-derived iPS. Secondary myelofibrosis (SMF) iPS established from a patient with SMF and primary myelofibrosis (PMF) iPS established from a patient with PMF on mouse embryo fibroblast feeder cells are shown here. Original magnification ratio: ×40. White bar = 0.1 mm. (**B**) Immunofluorescence staining of pluripotency marker antigens (SSEA-4 and Tra-1-60) on MF-iPS. (**C**) Semiquantitative reverse transcription polymerase chain reaction of pluripotency markers. Endogenous expression of pluripotent stem cell specific genes was confirmed. (**D**) Semiquantitative reverse transcription polymerase chain reaction revealing exogenous expression of virally transduced reprograming factors in MF-iPS. (**E**) Histologic analyses of teratoma from MF-iPS. Formation of intestinal epithelium (upper left and right), cartilage and muscle (middle left), cartilage and vessel (middle right), and choroid (lower left and right). Hematoxylin and eosin staining. Original rate of magnification: ×100. (**F**) Bisulfite sequence analysis of NANOG gene promoter. *Black circles* represent methylated CpG, and white circles represent ummethylated CpG. CB-iPS = control iPS, PBMNC = peripheral blood mononuclear cells.

Disease marker status of MF-iPS

We then confirmed the disease-specific marker profiles of MF-iPS. The SMF sample had been diagnosed as JAK2 V617F mutation positive, and the primary myelofibrosis sample had a del(13) chromosome abnormality, which contained the RB1 gene region. Allele-specific PCR tests for JAK2 V617F mutation status of SMF-iPS revealed the existence of SMF-iPS with both JAK2 alleles mutated (V617F/V617F) and both JAK2 alleles normal (wt/wt) (Fig. 3A). These results were confirmed by direct sequence

analyses (Fig. 3B). For the PMF-iPS, fluorescence in situ hybridization analyses using probes on the deletion site were performed and revealed that all tested clones had the 13q deletion (Fig. 3C). The del(13) chromosome abnormality in PMF-iPS was confirmed by G-band karyotype analysis (Fig. 3D). Karyotype analysis of SMF-iPS revealed a normal karyotype (Fig. 3E).

Blood cell differentiation of MF-iPS

Next, we re-differentiated MF-iPS into blood cells. We performed re-differentiation by the previously reported "iPS sac" method for generating hematopoietic cells [17,18]. As a result, MF-iPS generated "saclike structures (iPS Sac)" and round-shaped cells, which morphologically looked like hematopoietic cells, immersed within the structures (Fig. 4A). A portion of these cells expressed CD34 and CD43, which are typical hematopoietic progenitor markers (Fig. 4B). SMF-iPS with the JAK2 V617F mutation and PMF-iPS tended to generate more $CD34^{+}43^{+}$ progenitor cells than SMF-iPS without the JAK2 mutation and normal iPS, although the difference was not statistically significant (Fig. 4C). Methylcellulose colony formation assay using the obtained $CD34^{+}CD43^{+}$ cells revealed an insignificant difference in generation of colony-forming units between MF-iPS and normal iPS (Fig. 4D). With differentiation medium supplemented with specific cytokines, these $CD34^{+}43^{+}$ progenitors derived from MF-iPS yielded erythroid lineage cells and myeloid lineage cells with surface antigen profiles similar to those of normal iPS (Fig. 4E, F).

Megakaryocyte generation from MF-iPS

We then differentiated MF-iPS-derived hematopoietic progenitors into megakaryocytes, one of the suspected sources of cytokines causing bone marrow fibrosis. The cells obtained showed the megakaryocyte markers CD41a and CD42b (Fig. 5A). $CD41a^{+}42b^{+}$ cells derived from MF-iPS contained megakaryocyte-like large cells with

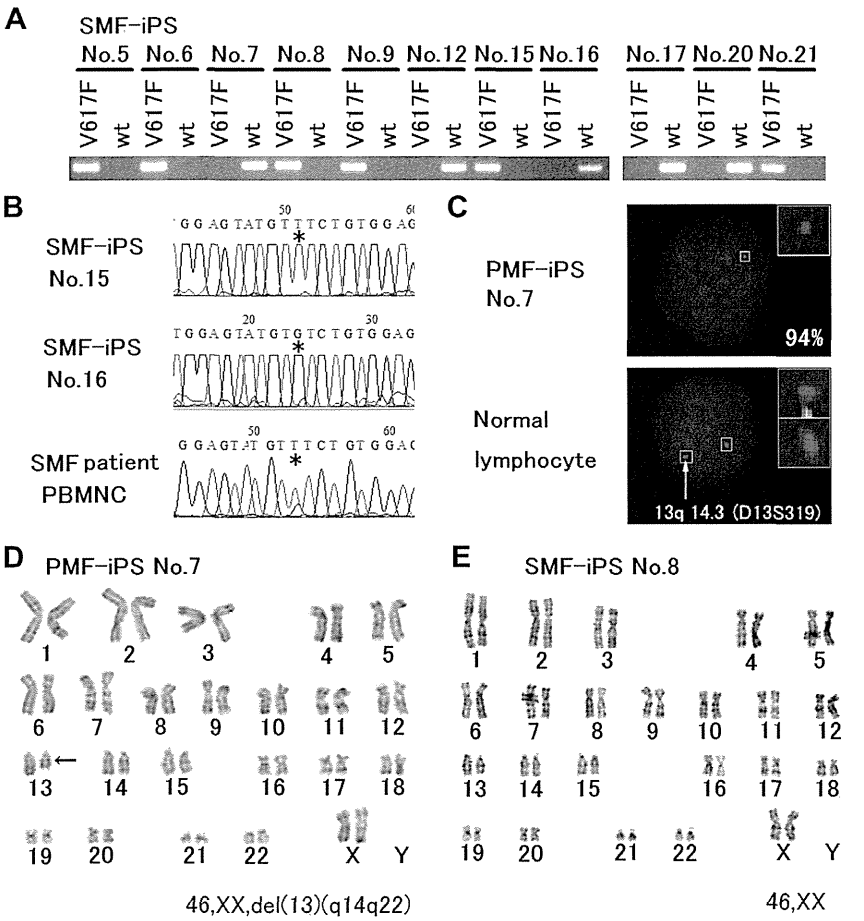

Figure 3. Disease-specific marker of myelofibrosis patient-derived induced pluripotent stem cells (iPS). (**A**) JAK2 allele-specific sequence of generated secondary myelofibrosis iPS (SMF-iPS). (**B**) Sequence analysis of SMF-iPS. (**C**) Fluorescence in situ hybridization reveals the 13q14.3 deletion of a primary myelofibrosis iPS (PMF-iPS). (**D**) Chromosome analysis of a PMF-iPS revealing del 13q. This result is representative of three lines tested. (**E**) Chromosome analysis of a SMF-iPS revealing normal karyotype. This result is representative of two lines tested. PBMNC = peripheral blood mononuclear cells.

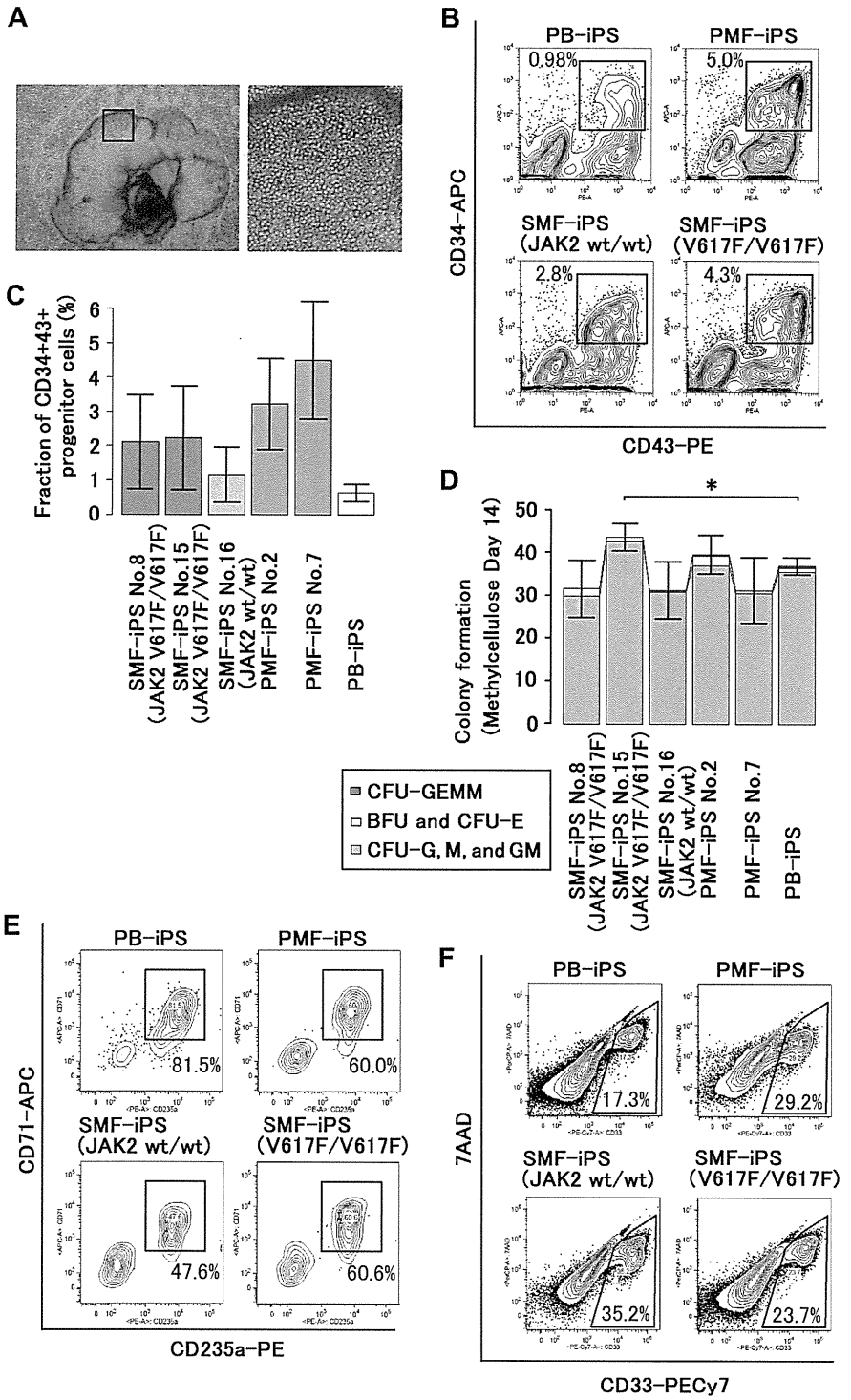

Figure 4. Hematopoietic cell differentiation of myelofibrosis patient-derived induced pluripotent stem cells (iPS). (**A**) Secondary myelofibrosis (SMF) iPS sac on day 14 of co-culture. Many bloodlike round-shaped cells were observed in the "iPS sac." (**B**) Surface markers of MF-iPS-derived progenitor cells. Cells co-expressing an immature blood cell marker CD43 and hemogenic epithelium and a hematopoietic progenitor marker CD34 were observed. (**C**) Efficiency of hematopoietic differentiation of MF-iPS. Fractions of progenitor cells at sorting on day 15 of co-culture are shown. Error bars represent standard deviations (n = 3). (**D**) Numbers of colony-forming units (CFUs) in 2400 sorted $CD34^{+}43^{+}$ progenitor cells on day 15 of co-culture. Error bars represent standard deviations of total colony numbers (n = 3). *$p < 0.05$. (**E**) Surface markers of erythroid cells differentiated from MF-iPS. Flow cytometry. (**F**) Surface markers of myeloid cells differentiated from MF-iPS. Flow cytometry.